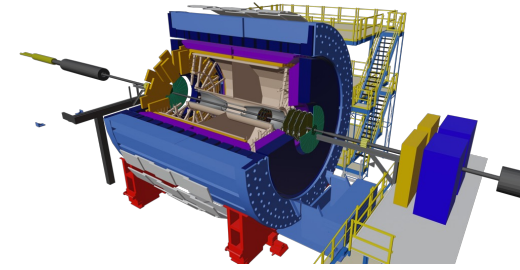
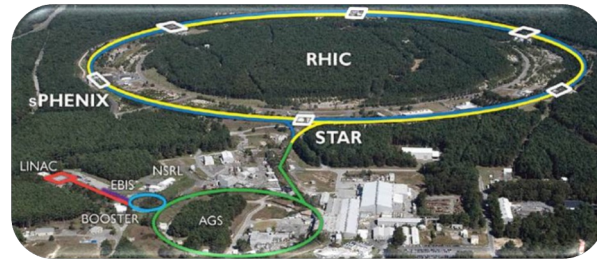


Supported by



U.S. DEPARTMENT OF
ENERGY

Office of
Science



Measurements of Hypernuclei Properties and Production at STAR

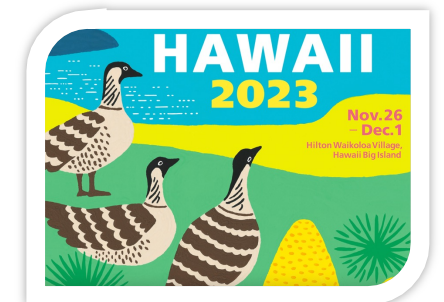
Yuanjing Ji

for the STAR collaboration

Lawrence Berkeley National Laboratory



DNP APS-JPS 2023



Outline

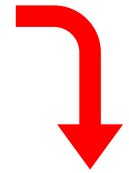


- Introduction
- The STAR experiment
- Hypernuclei measurements at STAR
 - Hypernuclei properties
 - Hypernuclei production and collectivity
- Summary and Outlook

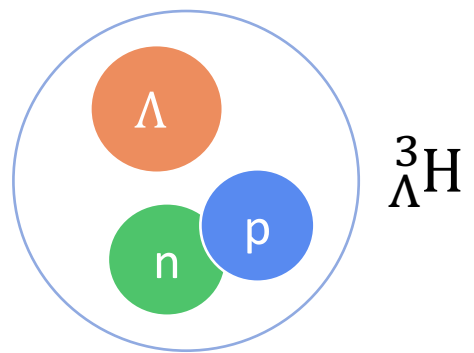
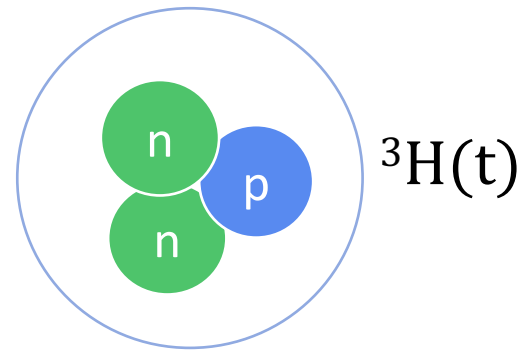
What are Hypernuclei?

Hypernucleus: A bound system of nucleons with ≥ 1 hyperon.

Hyperon: A baryon with ≥ 1 strange quark (e.g. Λ , Ξ , Ω etc).



Additional dimension in chart of nuclides



lightest hypernucleus

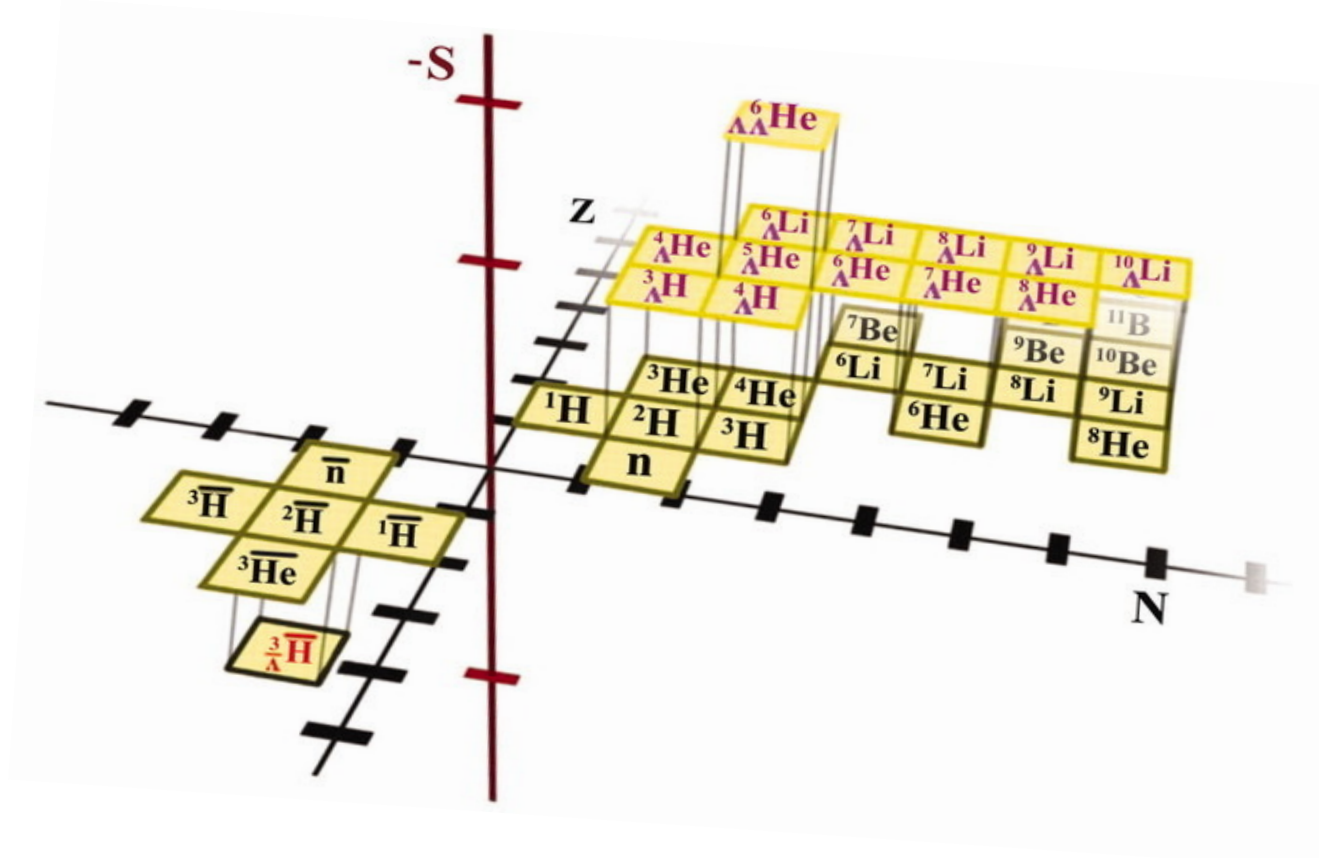
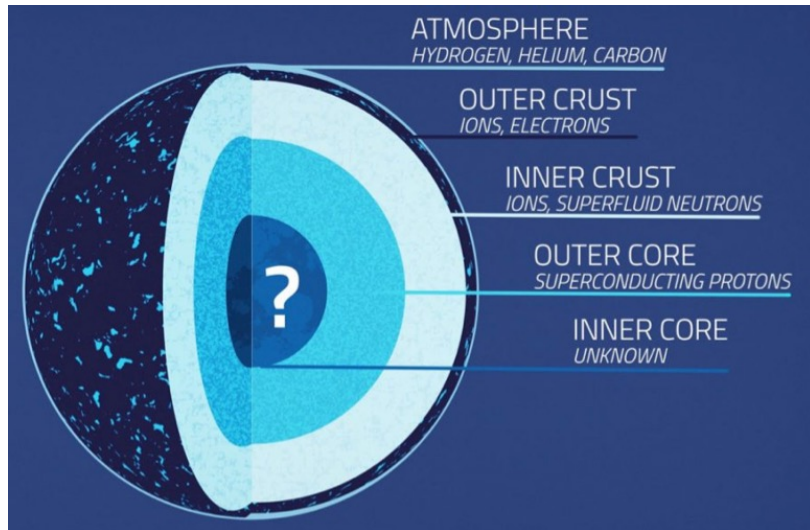


Figure from Science 328 (2010) 58-62

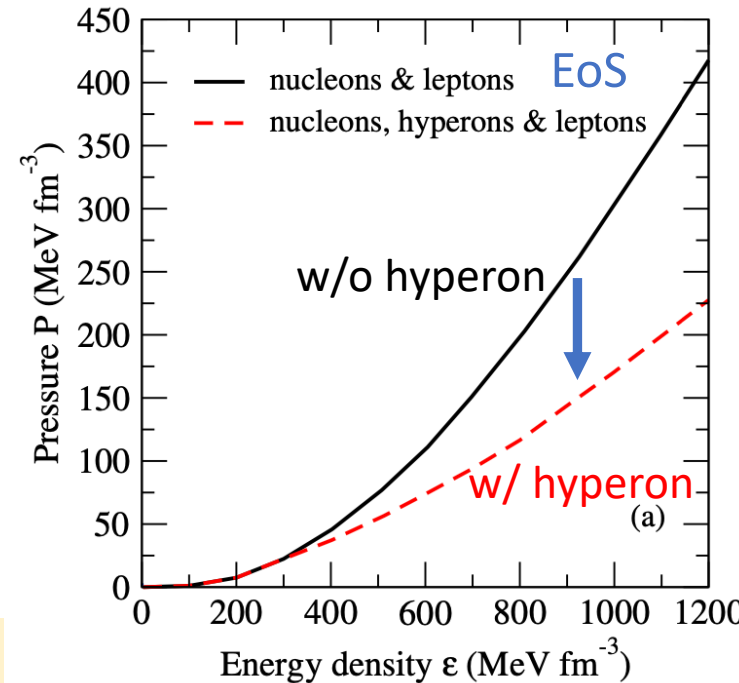
Y-N interaction and Astrophysics

Hypernucleus: Introduce additional degree of freedom in baryon interactions.

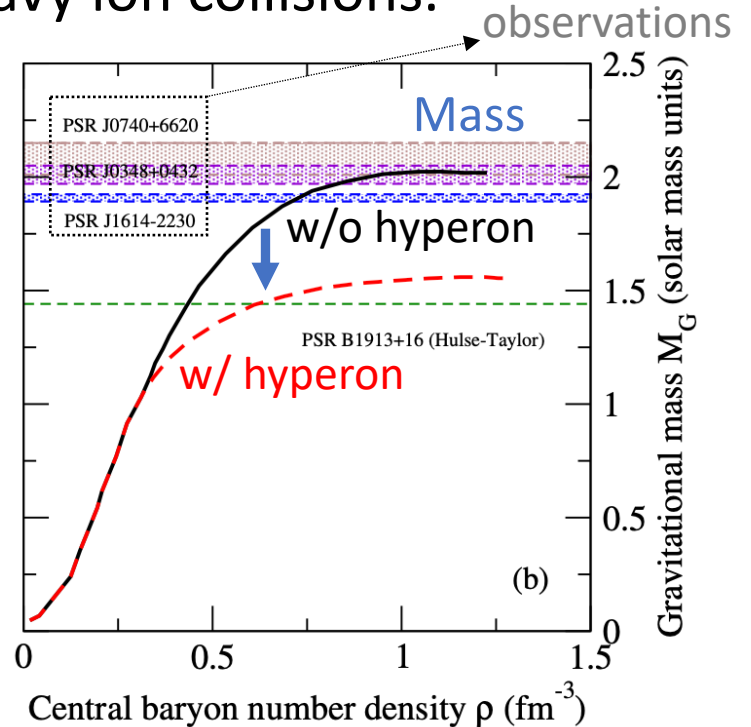
- Investigate **Hyperon-Nucleon (Y-N) interactions** in the nuclear experiments.
 - Constrain the strangeness degree of freedom of Equation of State (EoS).
 - e.g. EoS of **neutron stars** and hadronic phase of heavy ion collisions.



- EoS governs the structure of neutron stars.

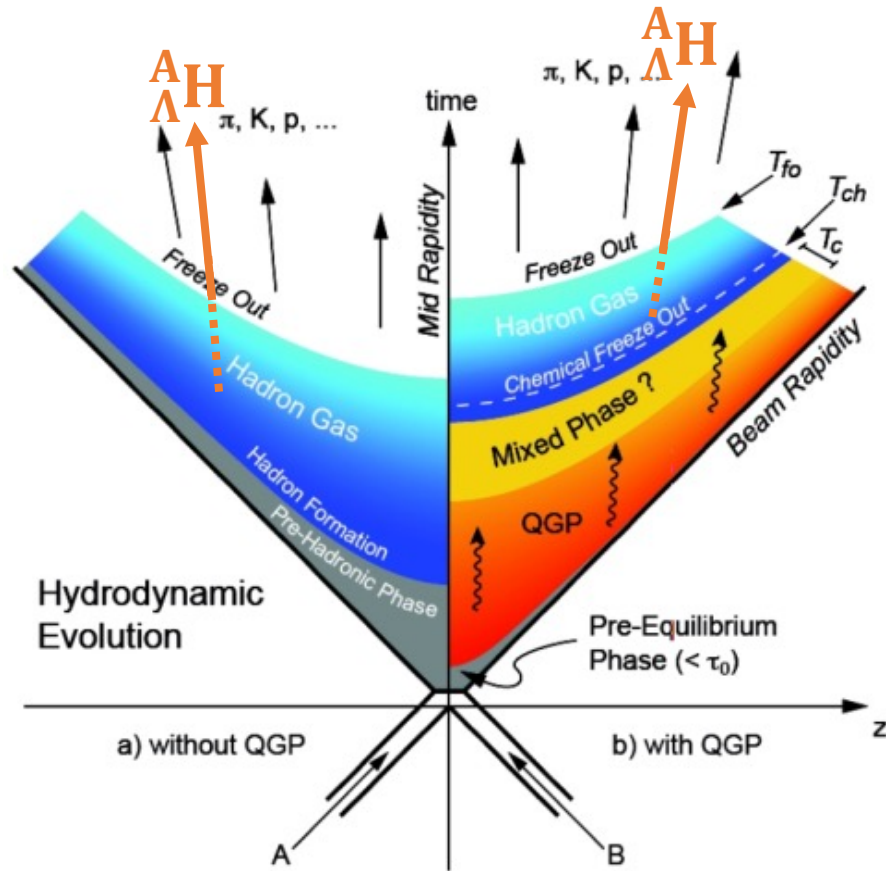


PSR J1614-2230: Nature 467,1081 (2010)
 PSR J0348+0432: Science 340, 1233232 (2013)
 PSR J0740+6620: Nature Astronomy 10,1038 (2019)



EPJ Web Conf. 271 (2022) 09001
 Eur. Phys. J. A (2016) 52: 29

Hypernuclei in Heavy ion Collisions



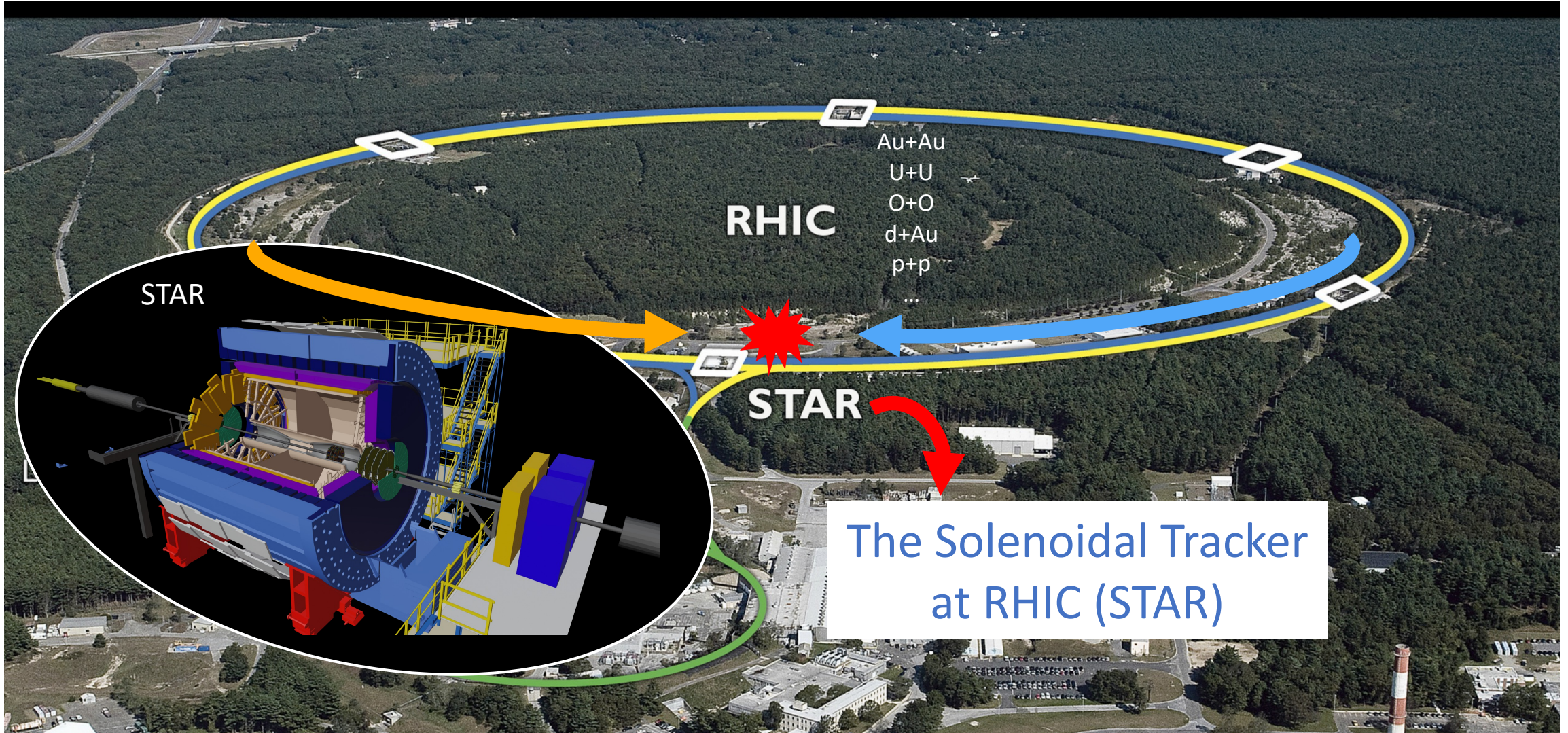
Observables:

- Intrinsic properties.
 - Lifetime, binding energy, branching ratio.
- Production yields.
- Collective flow.

Research focus:

- Hyperon-Nucleon (Y-N) interactions.
- EoS of dense nuclear matter at high μ_B .
- Production mechanisms.

RHIC and The STAR Detector



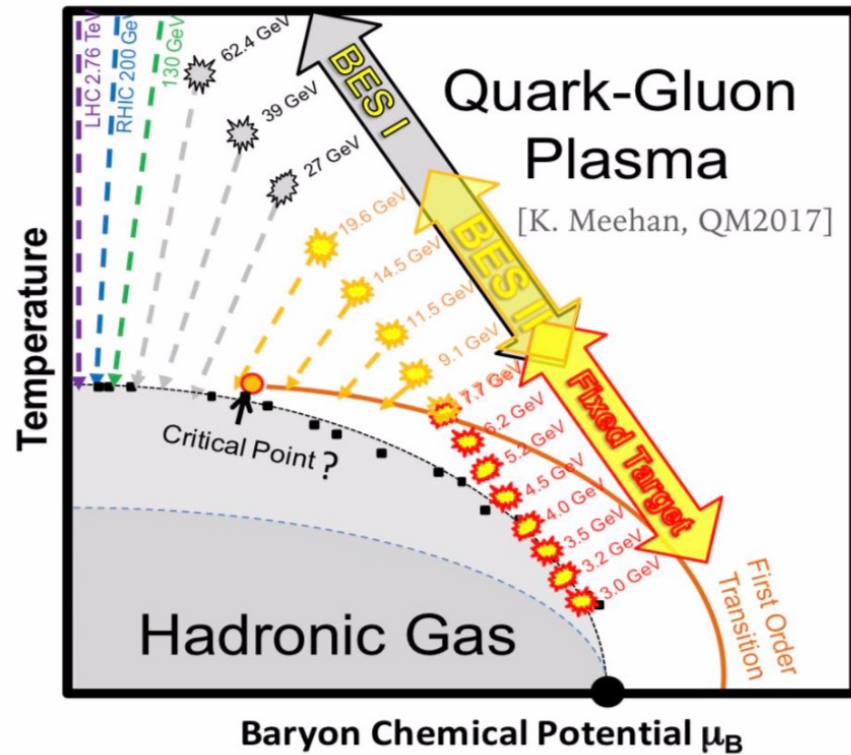
STAR Beam Energy Scan II Program (BES II)



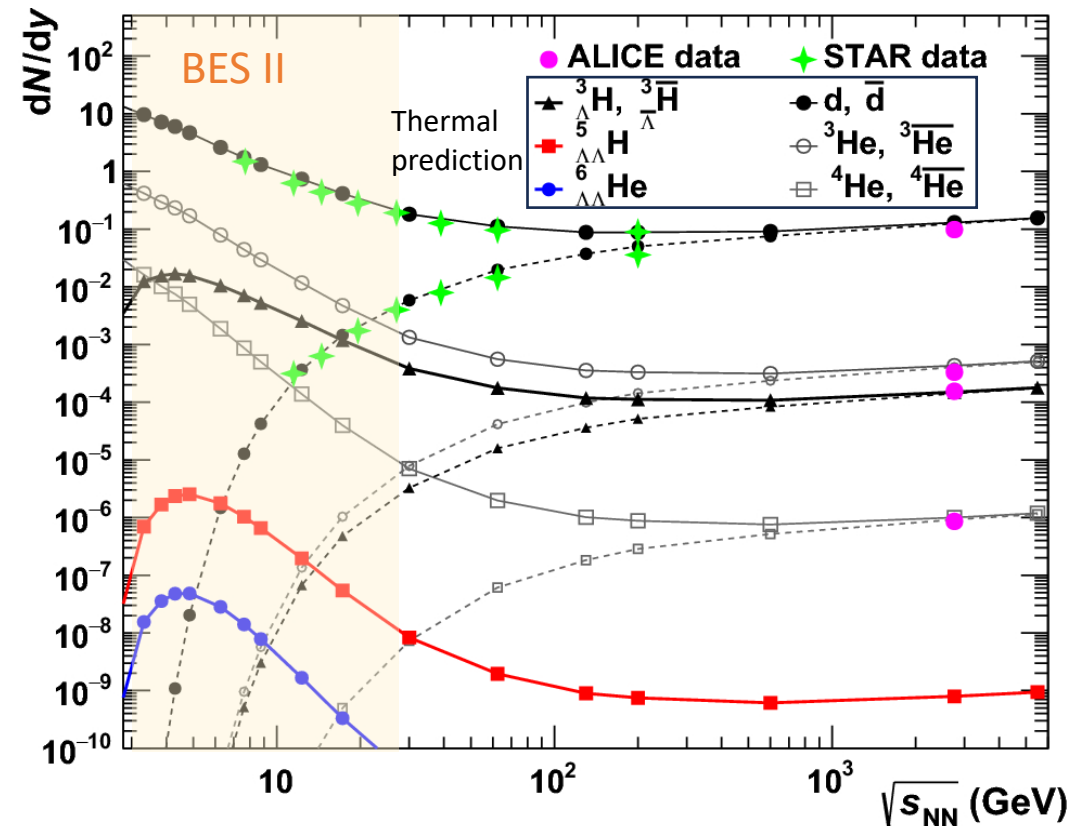
- Mapping the QCD diagram in the region of $200 < \mu_B \leq \sim 720$ MeV.
 - Collisions species: Au+Au.
 - Collider mode: $\sqrt{s_{NN}} = 7.7 - 27$ GeV.
 - Fixed-Target mode: $\sqrt{s_{NN}} = 3.0 - 7.7$ GeV
 - High collision rates.

Opportunities:

Abundant production of hypernuclei at BES II energies!



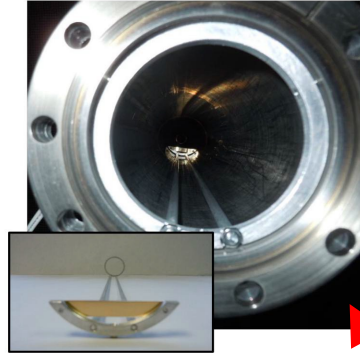
Thermal model predictions



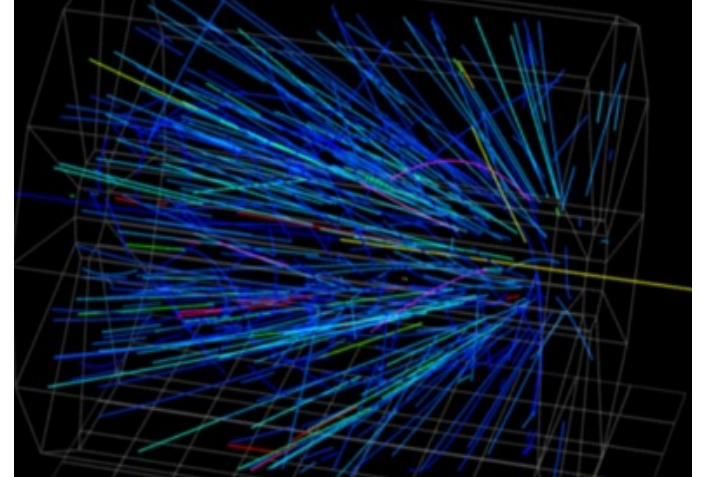
Fixed-Target Setup at STAR



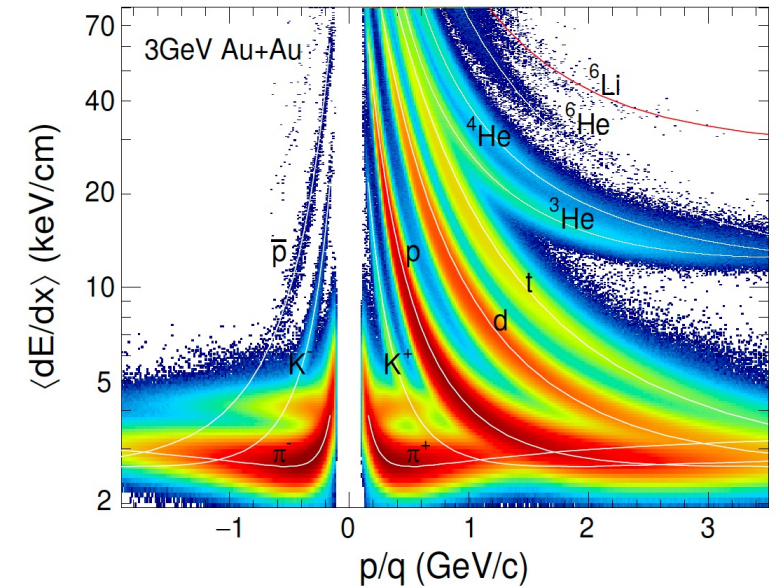
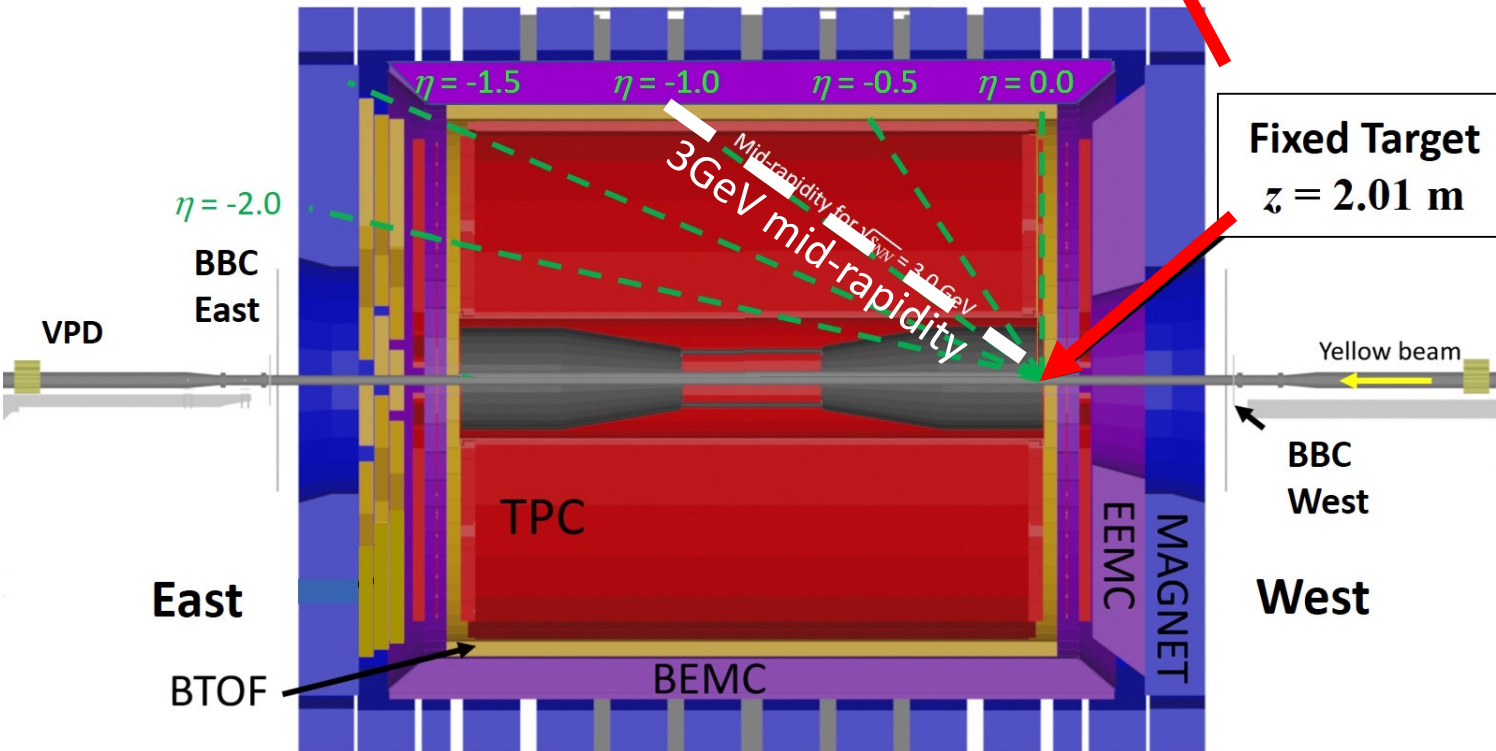
Gold foil,
250 μm thick



STAR Event Display (FXT)
Au+Au $\sqrt{s_{NN}} = 3 \text{ GeV}$



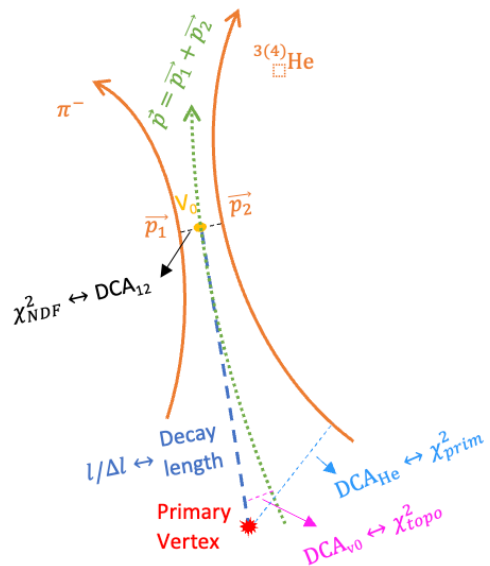
Fixed Target
 $z = 2.01 \text{ m}$



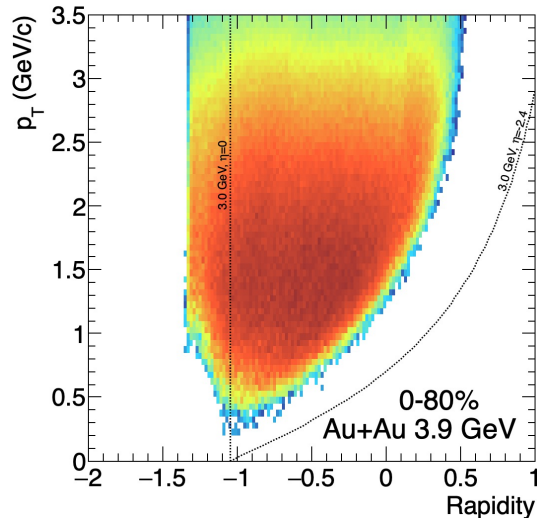
Signal reconstruction



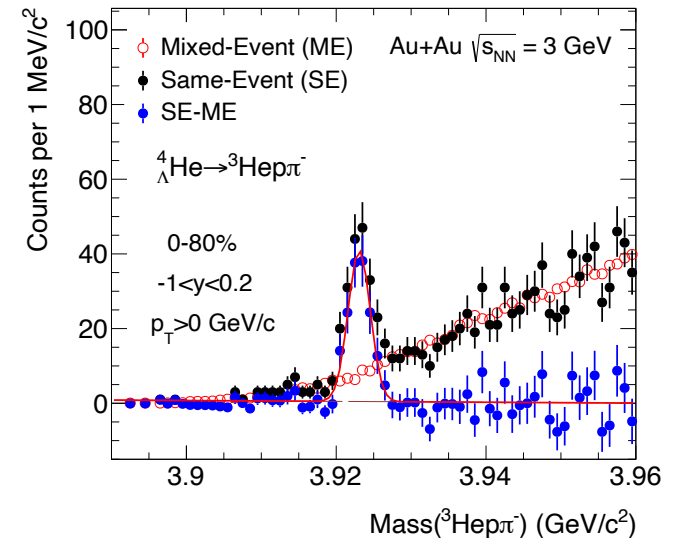
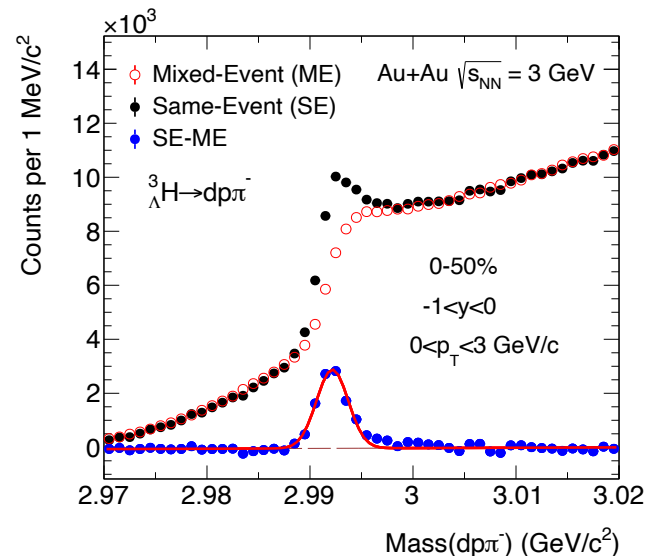
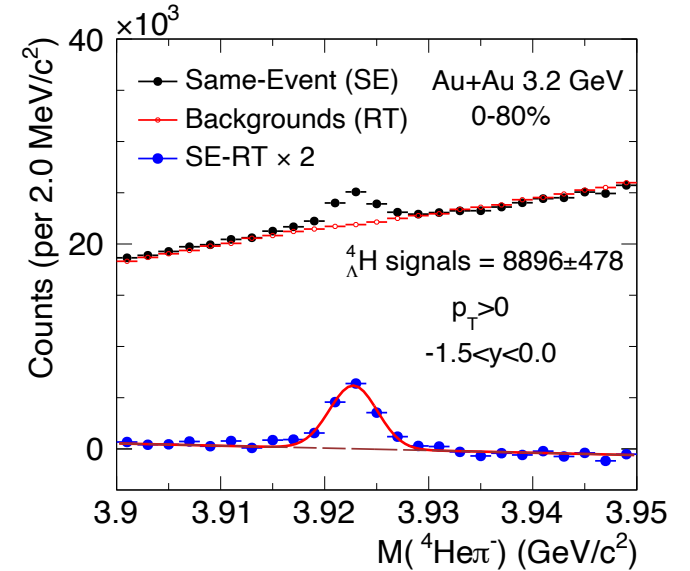
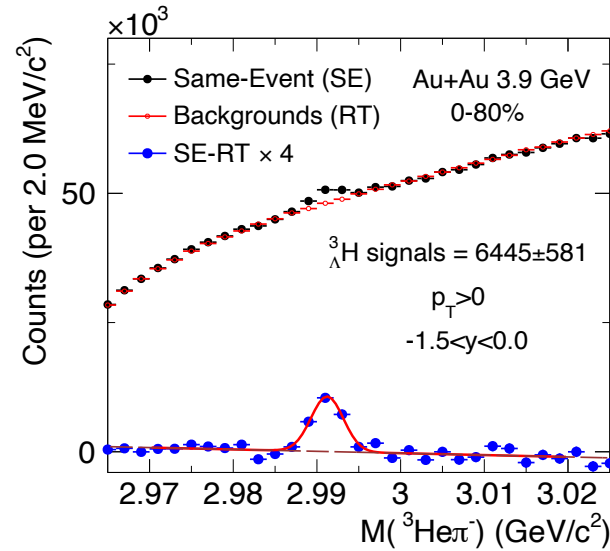
- Decay channel:
 - ${}^3_{\Lambda}\text{H} \rightarrow {}^3\text{He} \pi^- \sim \text{B.R. } 20\text{-}25\%$,
 - ${}^4_{\Lambda}\text{H} \rightarrow {}^4\text{He} \pi^- \sim \text{B.R. } 50\%$,
 - ${}^3_{\Lambda}\text{H} \rightarrow \text{dp} \pi^- \sim \text{B.R. } \sim 40\text{-}50\%$,
 - ${}^4_{\Lambda}\text{He} \rightarrow {}^3\text{He} \text{p} \pi^- \sim \text{B.R. } \sim 23\%$
- Backgrounds reconstructed by rotation of ${}^3(4)\text{He}$.



2-body decay topology

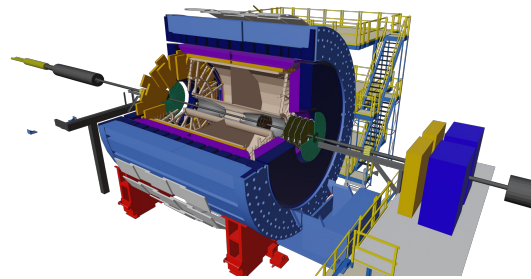
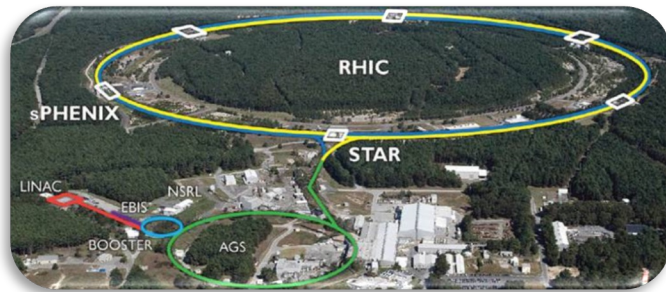


Acceptance of ${}^3_{\Lambda}\text{H}$ (from MC)





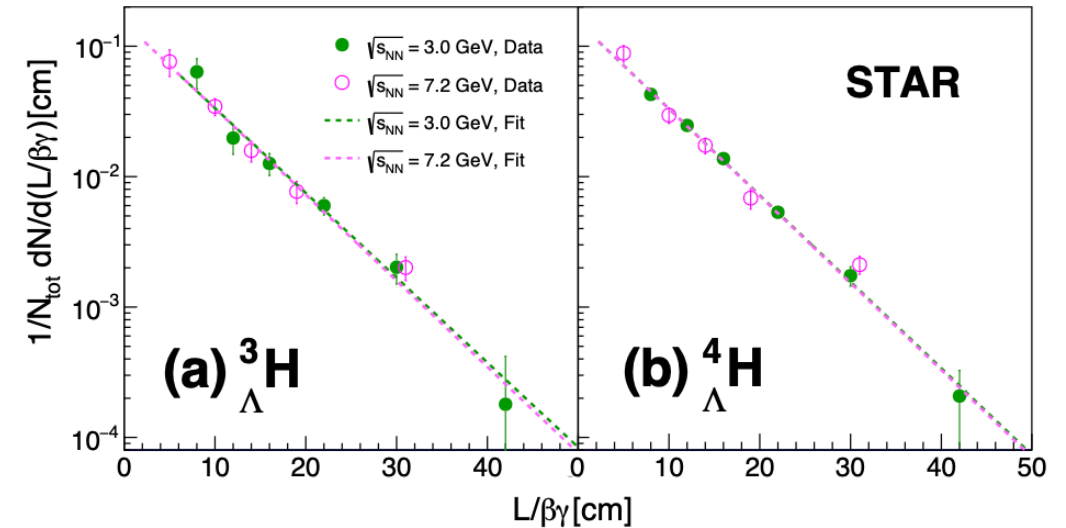
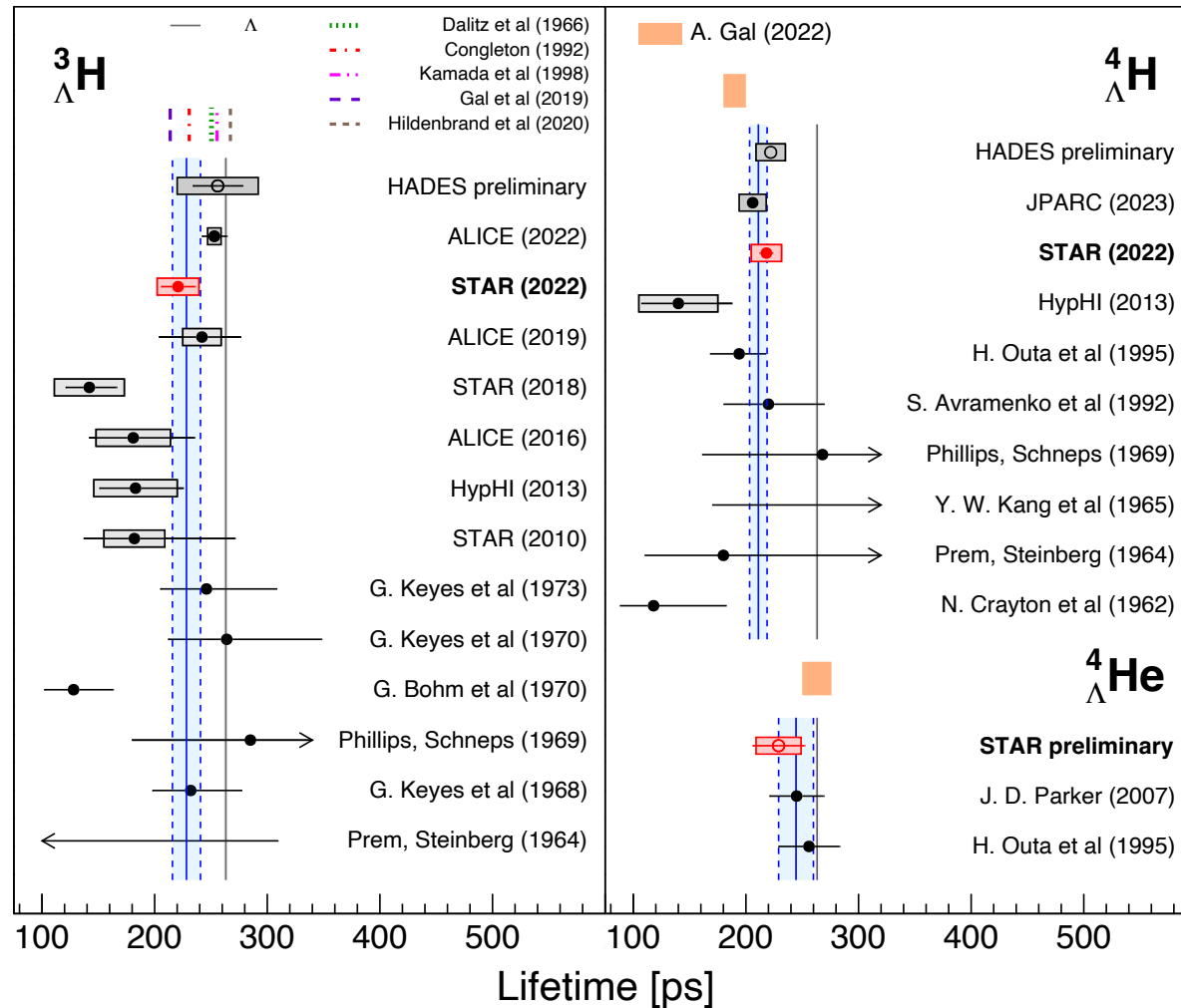
Measurements of Hypernuclei Properties at STAR



Hypernuclei Lifetimes



${}^3_{\Lambda}\text{H}$, ${}^4_{\Lambda}\text{H}$ lifetime: STAR, PRL 128, 202301 (2022)



A. Gal et al, PLB791, 48 (2019)

${}^3_{\Lambda}\text{H}$: Global avg. = $(87 \pm 5)\% \tau(\Lambda)$, $2.8\sigma < \tau(\Lambda)$.

- Calculations with pion FSI consistent with data.

${}^4_{\Lambda}\text{H}$, ${}^4_{\Lambda}\text{He}$: $\tau({}^4_{\Lambda}\text{H})/\tau({}^4_{\Lambda}\text{He}) = 0.86 \pm 0.06$.

- Lifetime ratio consistent with calculation based on isospin rule.

A. Gal, EPJ Web Conf. 259, 08002 (2022) $\frac{\Gamma({}^4_{\Lambda}\text{He} \rightarrow {}^4\text{He} + \pi^0)}{\Gamma({}^4_{\Lambda}\text{H} \rightarrow {}^4\text{He} + \pi^-)} \approx \frac{1}{2}$



${}^3_{\Lambda}\text{H}$ Branching Ratio R_3

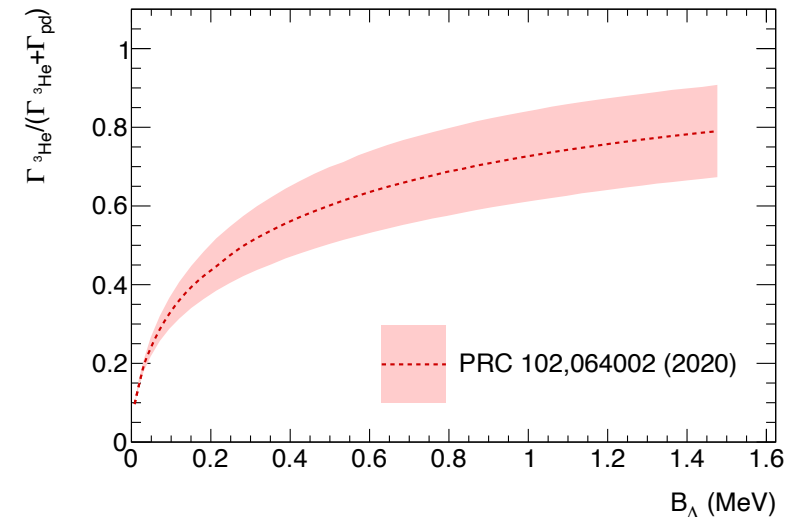
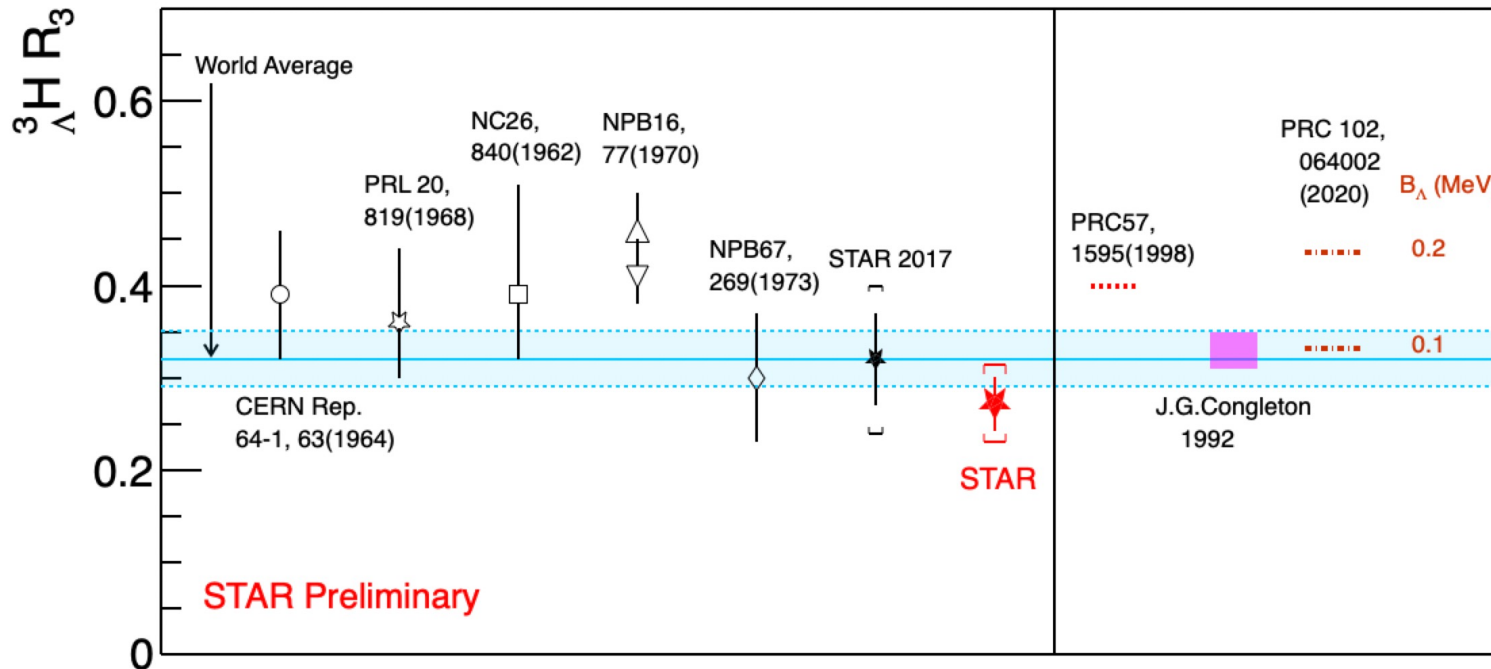
Improved precision on R_3 .

- Stronger constraints on absolute B.R. and hypertriton internal structure models.
- **Model comparison show data favors small B_{Λ} .**

$$R_3 = \frac{\text{B. R. } ({}^3_{\Lambda}\text{H} \rightarrow 3\text{He}\pi^-)}{\text{B. R. } ({}^3_{\Lambda}\text{H} \rightarrow \text{pd}\pi^-) + \text{B. R. } ({}^3_{\Lambda}\text{H} \rightarrow 3\text{He}\pi^-)}$$

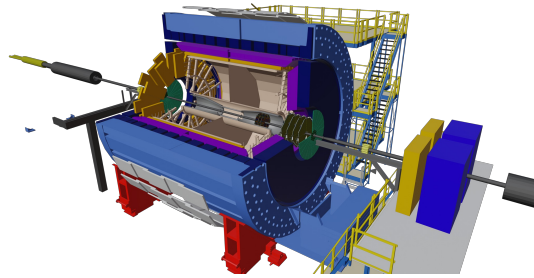
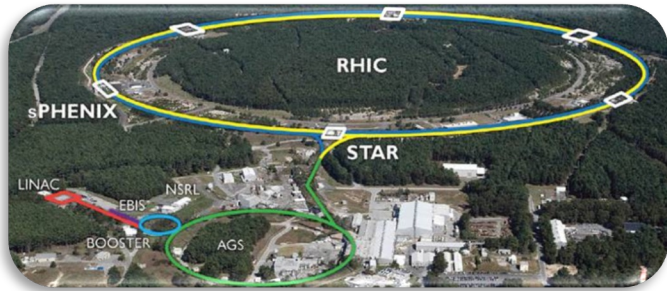
STAR: $R_3 = 0.272 \pm 0.030 \pm 0.042$

Updated world average: **0.32 ± 0.03**





Hypernuclei Production and Collectivity in Au+Au Collisions



Hypernuclei production mechanism in HIC



- **When and how loosely bound hypernuclei are formed in HIC?**

$${}^3_{\Lambda}\text{H } B_{\Lambda} \sim 0.07\text{-}0.4 \text{ MeV}, T_{ch} \gg B_{\Lambda}$$

- **Formation mechanism can be classified as:**

- **Coalescence formation**

- Dominates at **mid-rapidity**.

- Baryons / nuclei very close in phase space (\vec{p}, \vec{r}) .

- **Nuclear fragmentation of hypercluster**

- Dominates at **beam rapidity**.

- Dominate for heavy hypernuclei formation.

- **Production models**

Thermal model

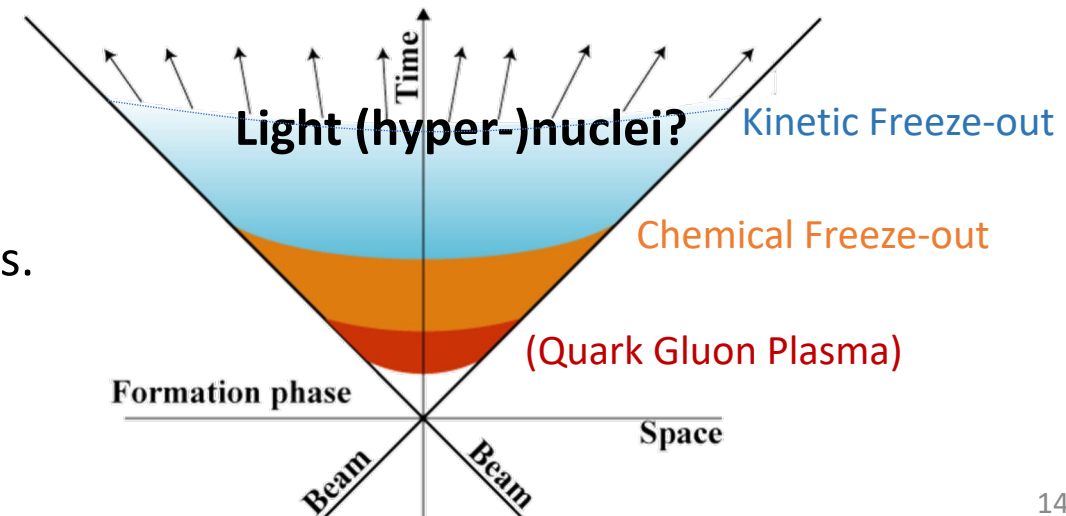
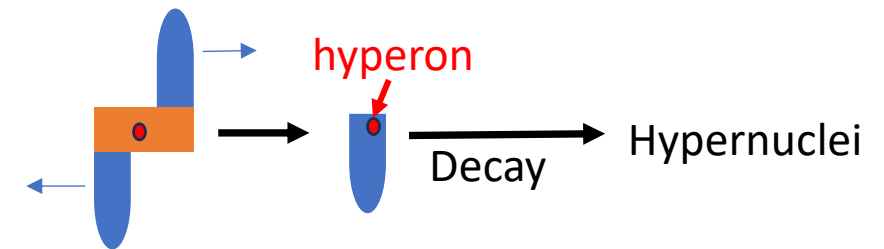
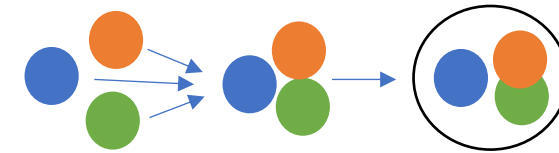
- Hadron **chemical freeze out** T_{ch} and μ_B .

Coalescence approach

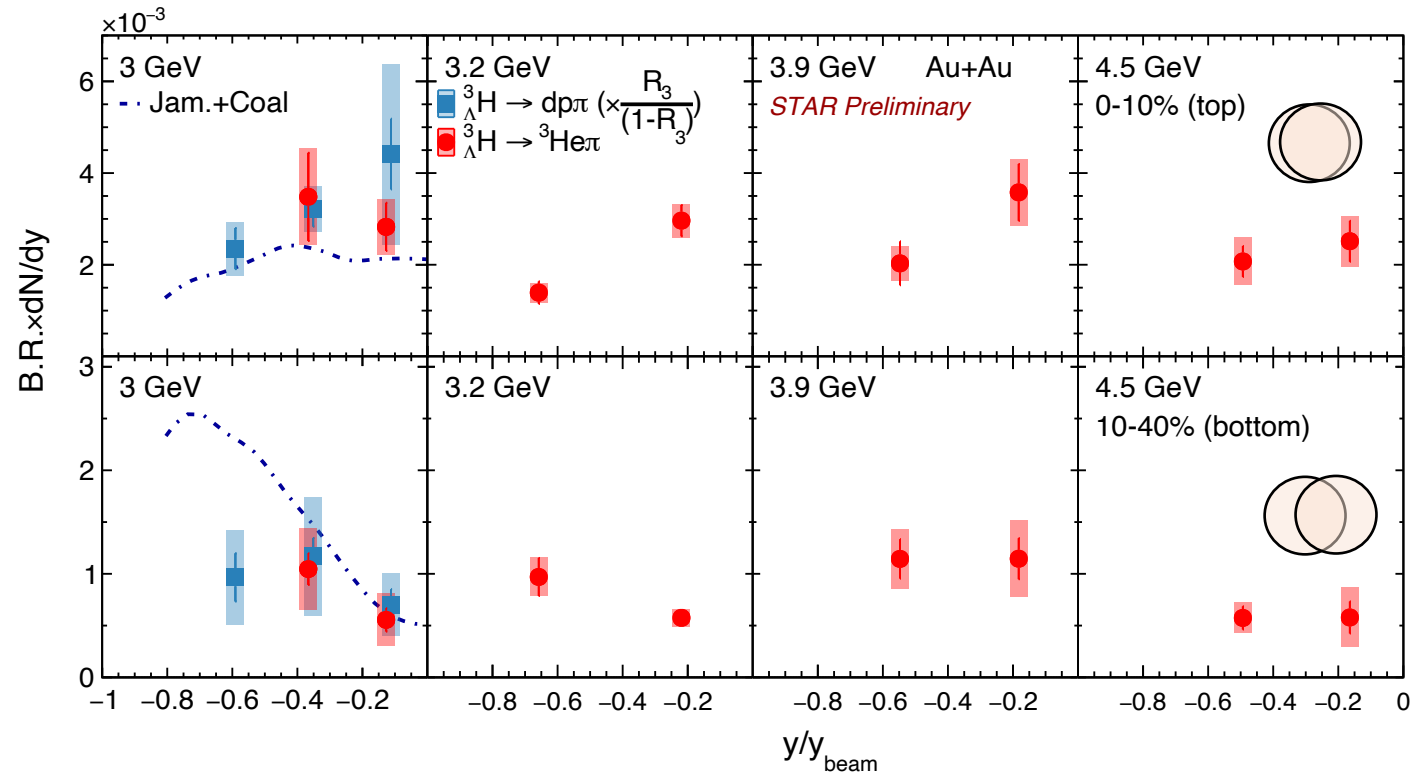
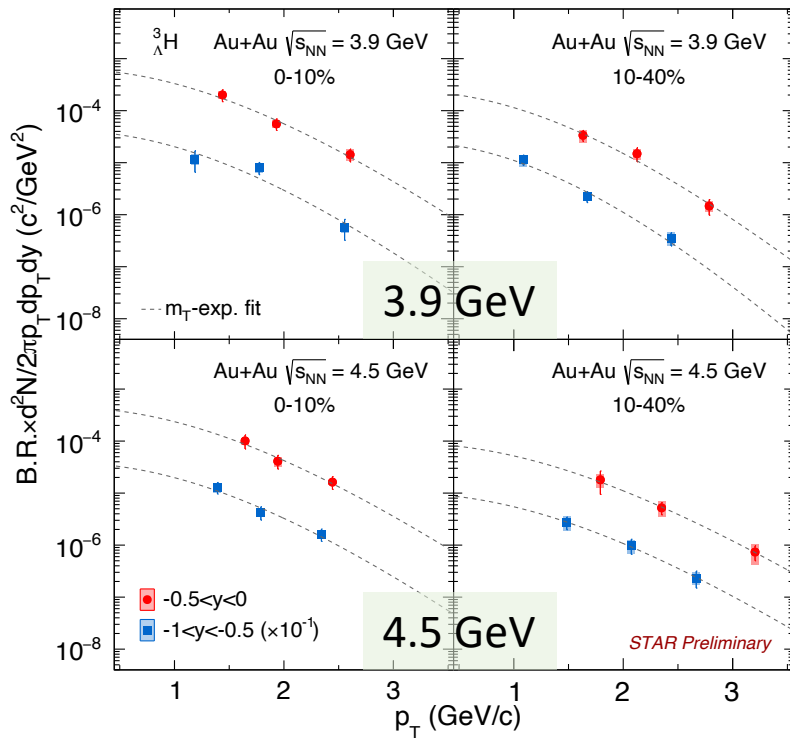
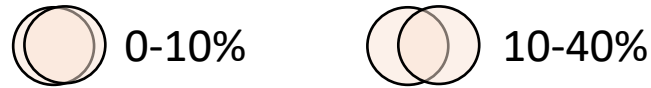
- Coalescence via final state interactions among nucleons.

Dynamical cluster formation

- Reaction-based; clusters can be formed before kinetic freeze-out.



${}^3_{\Lambda}\text{H}$ p_T Spectra, dN/dy in 3-4.5 GeV



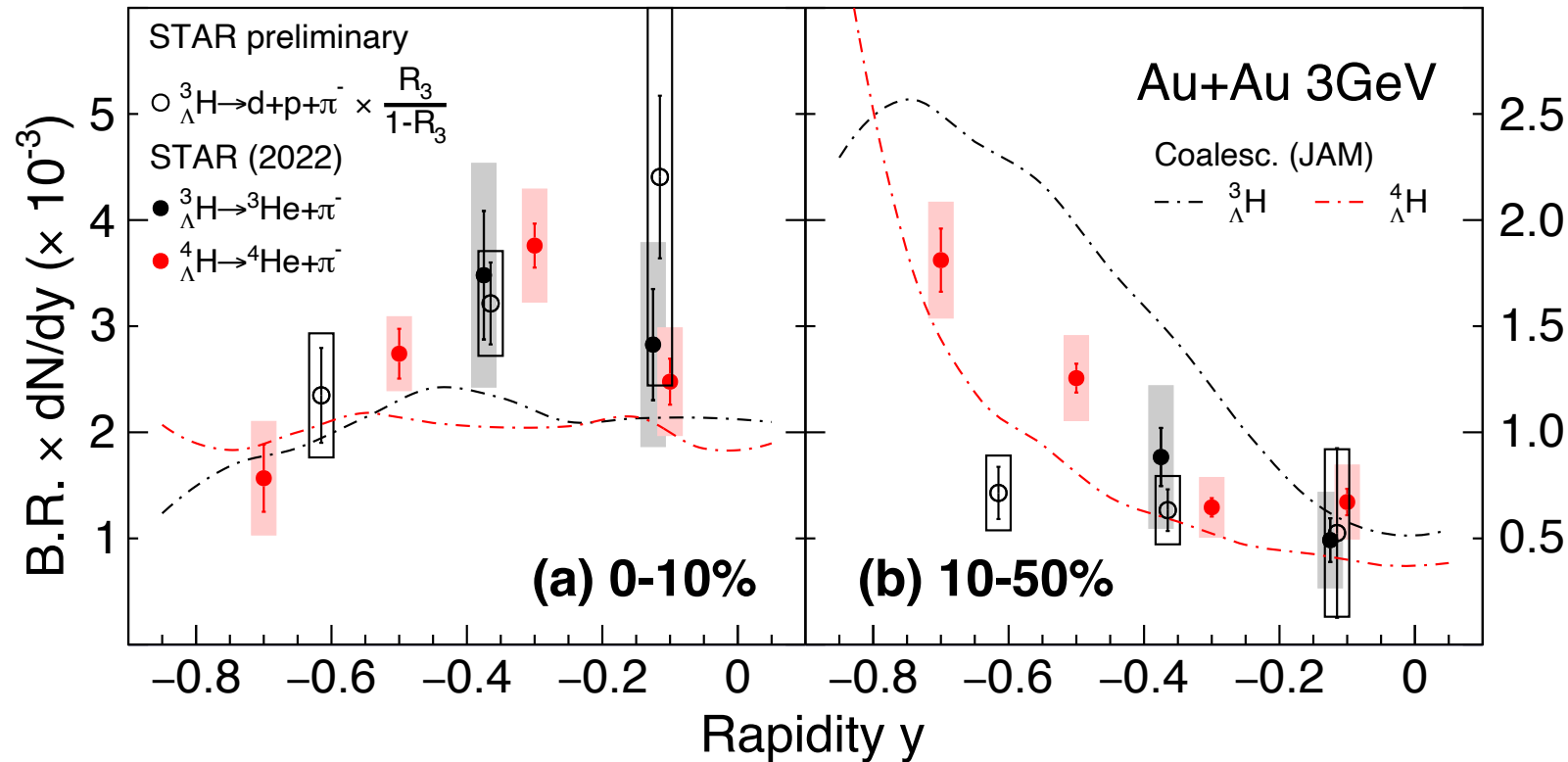
- Utilizing datasets collected by STAR Fixed-Target program, ${}^3_{\Lambda}\text{H}$ p_T spectra, dN/dy are measured at $\sqrt{s_{NN}} = 3-4.5$ GeV in Au+Au collisions.

${}^3_{\Lambda}\text{H}$ and ${}^4_{\Lambda}\text{H}$ dN/dy at 3 GeV



○ 0-10%

○ 10-50%

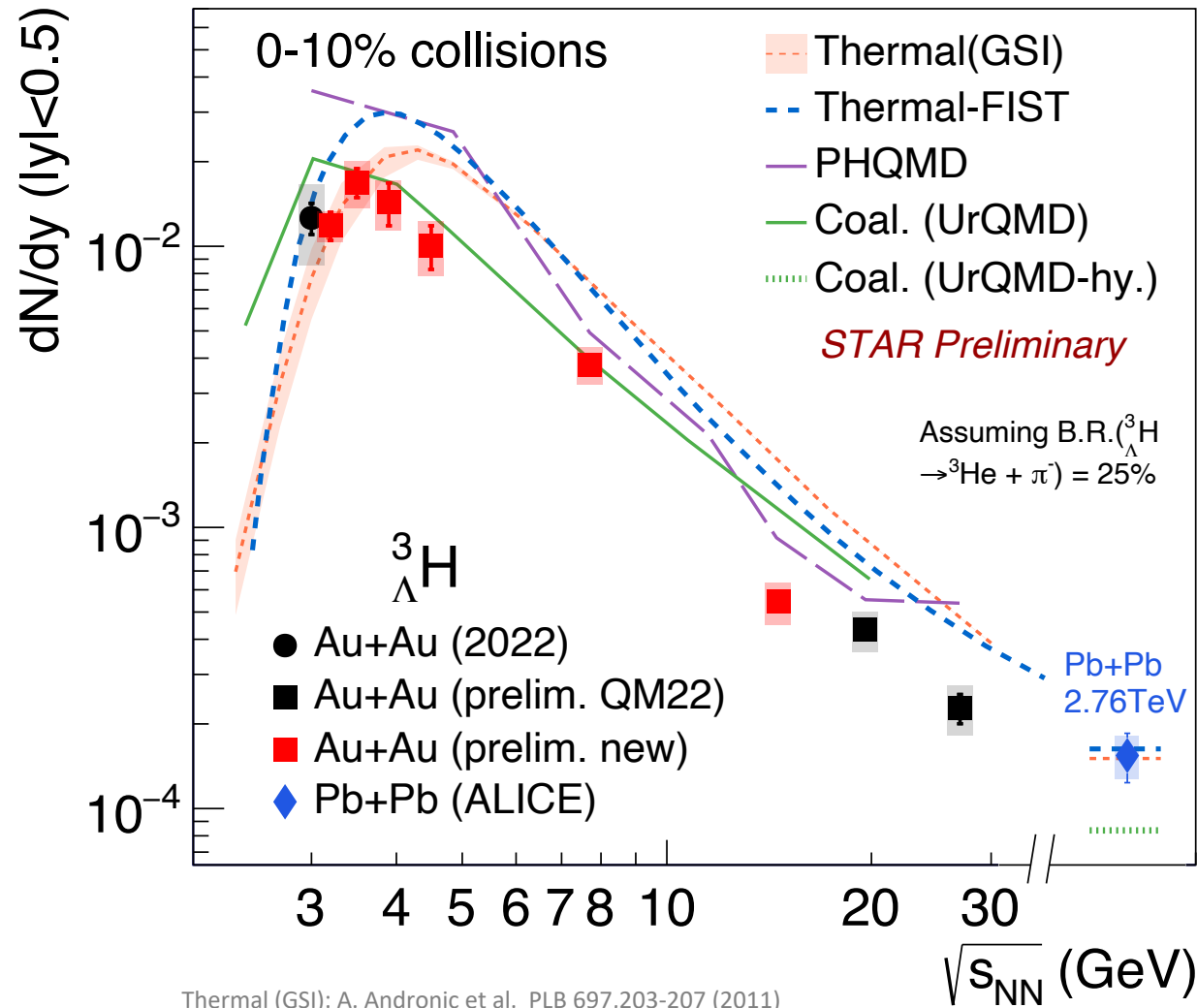


JAM+Coal.

- Tuned to match proton and Λ spectra from data;
- Instant coalescence after kinetic freeze-out
- Two body coalescence: d/t+ Λ

- Coalescence models with tuned parameters:
 - Qualitatively describe the trend of ${}^4_{\Lambda}\text{H}$ yields versus rapidity.
 - Fail to describe the ${}^3_{\Lambda}\text{H}$ tendency in 10-50% centralities.

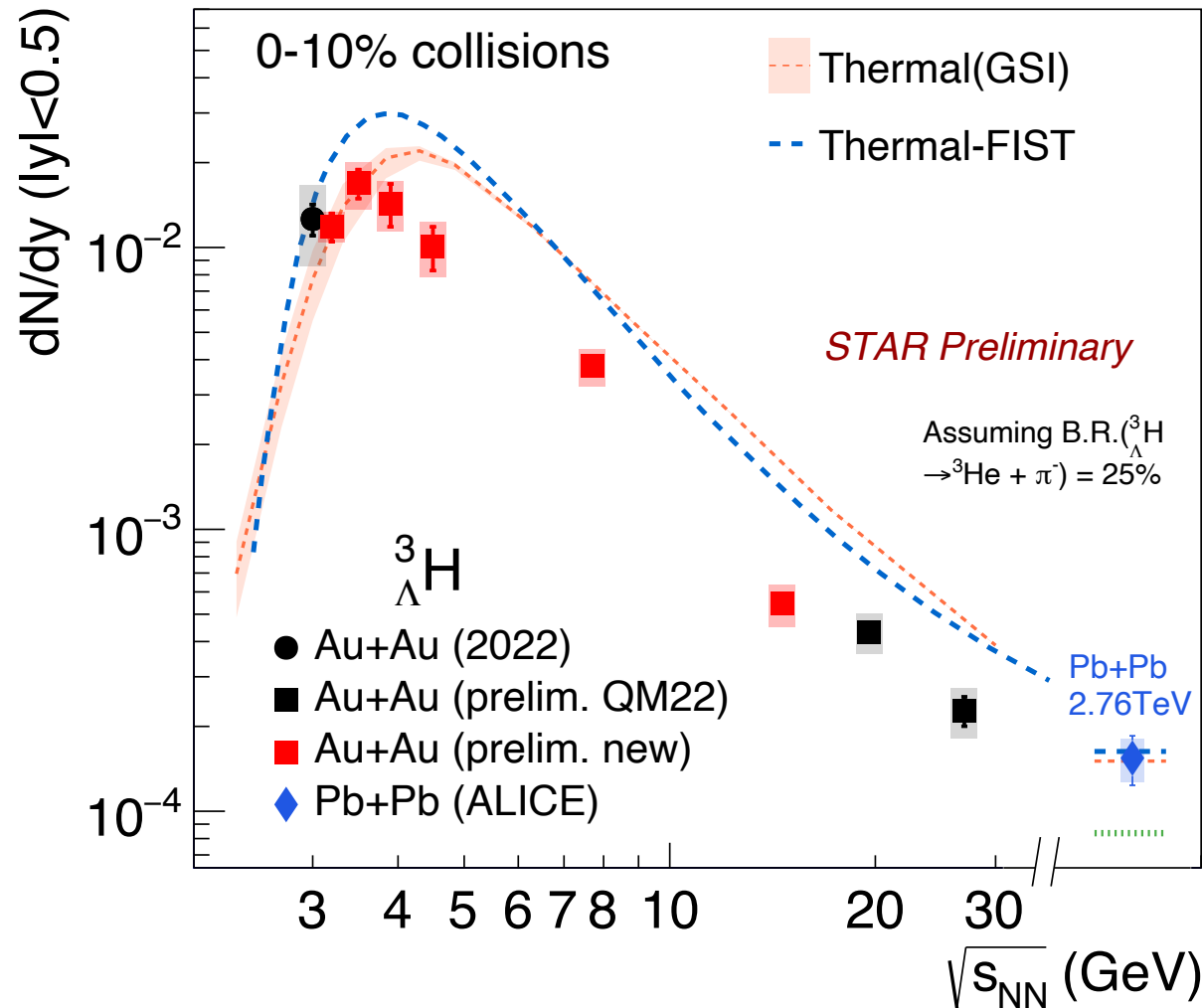
Energy Dependence of ${}^3_{\Lambda}\text{H}$ production



- ${}^3_{\Lambda}\text{H}$ yields peak at $\sqrt{s_{NN}} = 3-4$ GeV, then decrease toward higher energy.
 - Decreasing trend results from increasing baryon density at lower energies.

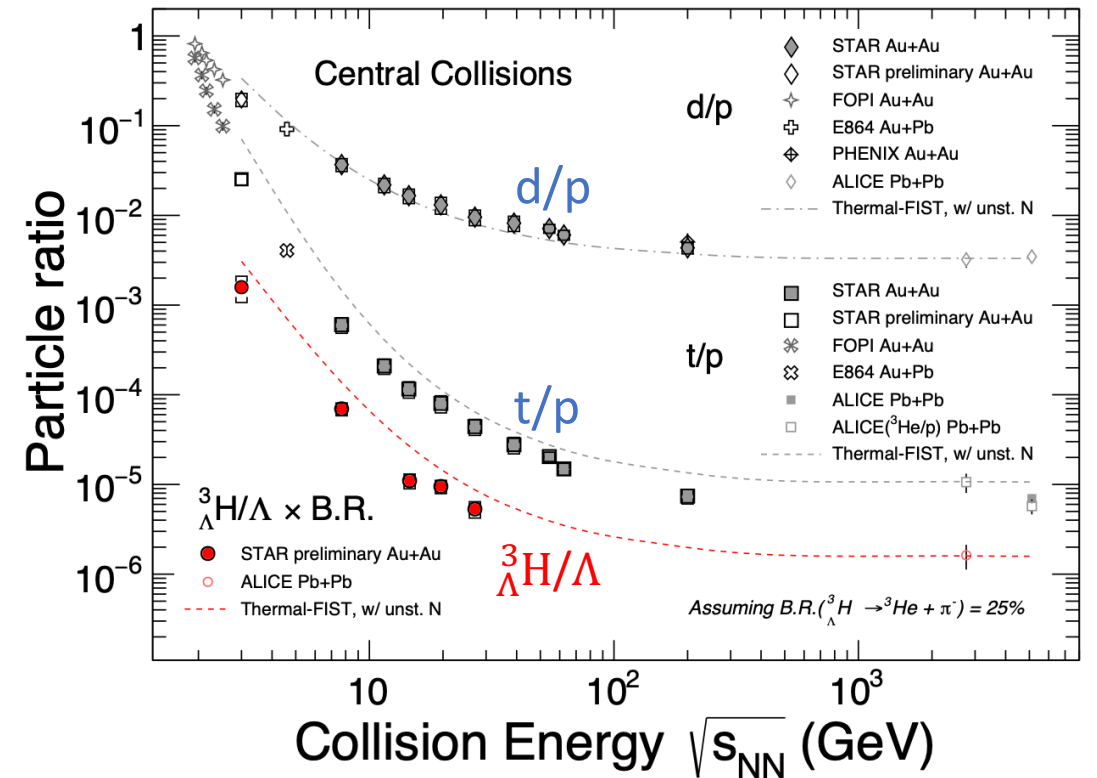
Thermal (GSI): A. Andronic et al. PLB 697,203-207 (2011)
 Thermal-FIST, Coal. (UrQMD): T. Reichert et al. PRC 107 (2023) 1, 014912
 PHQMD: S. Gläsel et al. PRC 105, 014908 (2022),
 V. Kireyeu et al. arXiv:1911.09496
 Pb+Pb: ALICE, PLB 754, 360 (2016)
 STAR at 3 GeV: PRL 128, 202301 (2022)

Energy Dependence of ${}^3_{\Lambda}\text{H}$ production



- Thermal model

- Hadron chemical freeze-out T and μ_B .

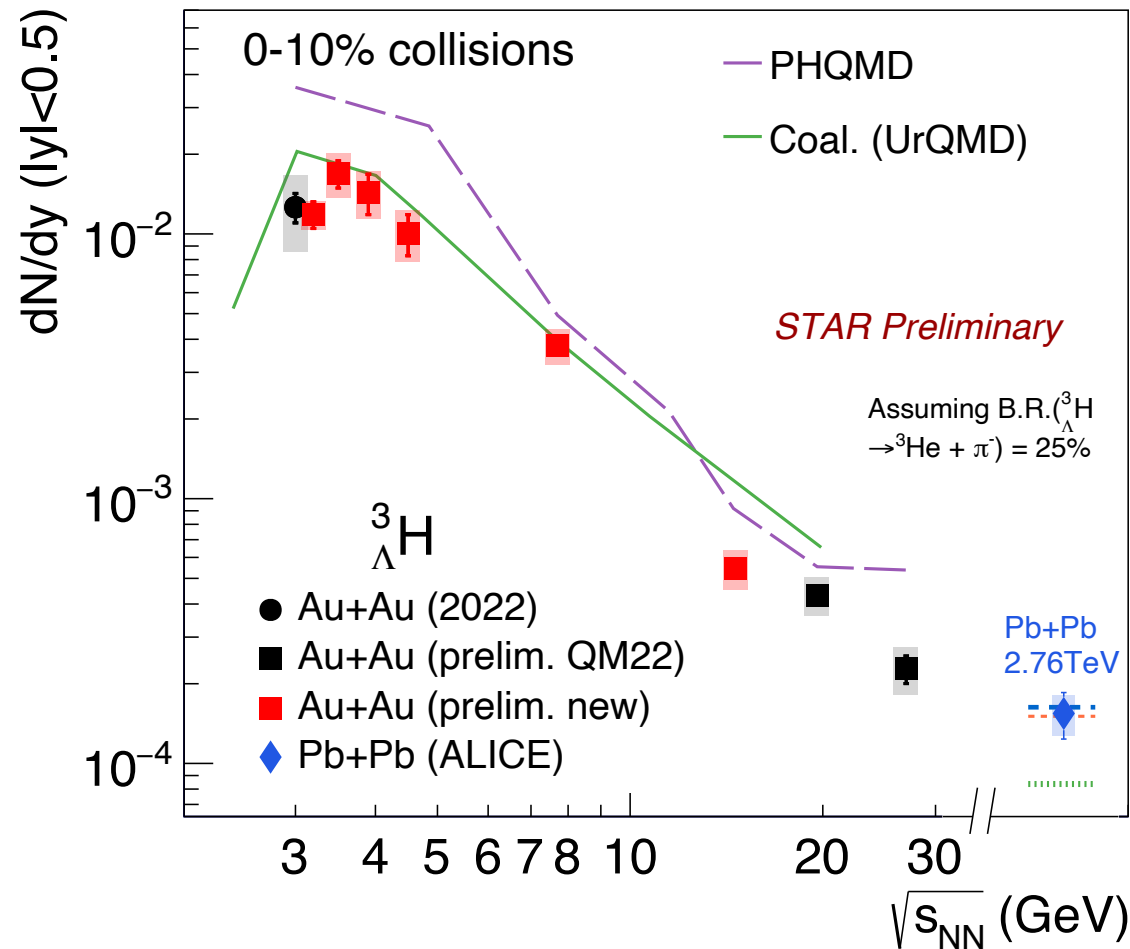


Thermal (GSI): A. Andronic et al. PLB 697,203-207 (2011)
 Thermal-FIST, Coal. (UrQMD): T. Reichert et al. PRC 107 (2023) 1, 014912
 PHQMD: S. Gläsel et al. PRC 105, 014908 (2022),
 V. Kireyeu et al. arXiv:1911.09496
 Pb+Pb: ALICE, PLB 754, 360 (2016)
 STAR at 3 GeV: PRL 128, 202301 (2022)

Hypernuclei yields are not fixed at hadron chemical freeze-out.

d/p and t/p: PRL 130 (2023) 202301

Energy Dependence of ${}^3_{\Lambda}\text{H}$ production



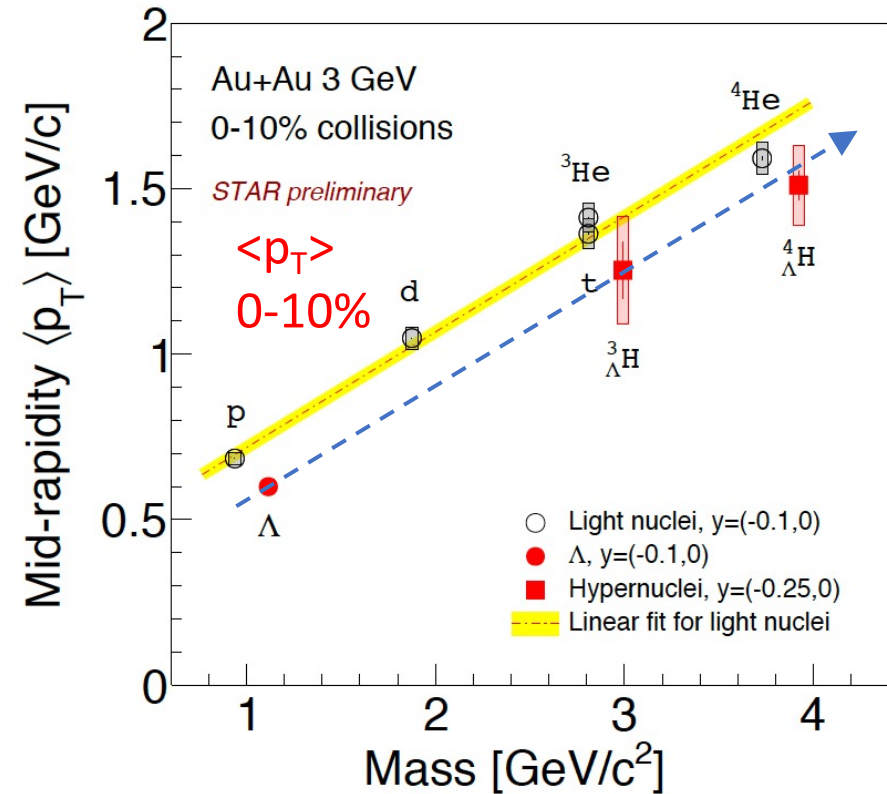
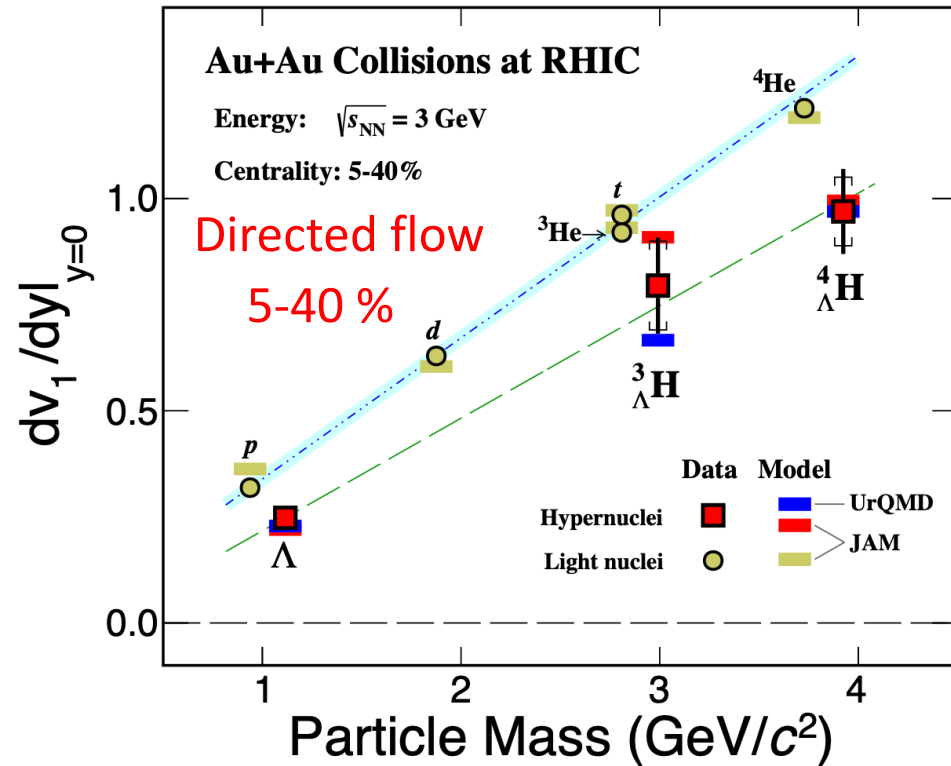
- **UrQMD + Coal.**
 - Instant coalescence after hadron kinetic freeze-out.
 - Coalescence condition:
 - $|\vec{p}_1 - \vec{p}_2| < \Delta P, |\vec{r}_1 - \vec{r}_2| < \Delta R.$
- **PHQMD**
 - Transport model + dynamical cluster formation.
 - Cluster can be formed before hadron kinetic freeze out.
 - Assuming $Y-N$ potential = $2/3 N-N$ potential.

Thermal (GSI): A. Andronic et al. PLB 697,203-207 (2011)
 Thermal-FIST, Coal. (UrQMD): T. Reichert et al. PRC 107 (2023) 1, 014912
 PHQMD: S. Gläsel et al. PRC 105, 014908 (2022),
 V. Kireyeu et al. arXiv:1911.09496
 Pb+Pb: ALICE, PLB 754, 360 (2016)
 STAR at 3 GeV: PRL 128, 202301 (2022)

• Strong constraints on model calculations!

Directed Flow (v_1) and $\langle p_T \rangle$ at 3 GeV

PRL 130 (2023) 212301



- v_1 slope following mass number scaling.

$$E \frac{d^3N}{dp^3} = \frac{1}{2\pi} \frac{d^2N}{p_T dp_T dy} \left(1 + \sum_1^{\infty} 2v_n \cos [n(\phi - \psi_{RP})] \right)$$

- Similar phenomena also seen in $\langle p_T \rangle$.
 - Radial flow contribution.

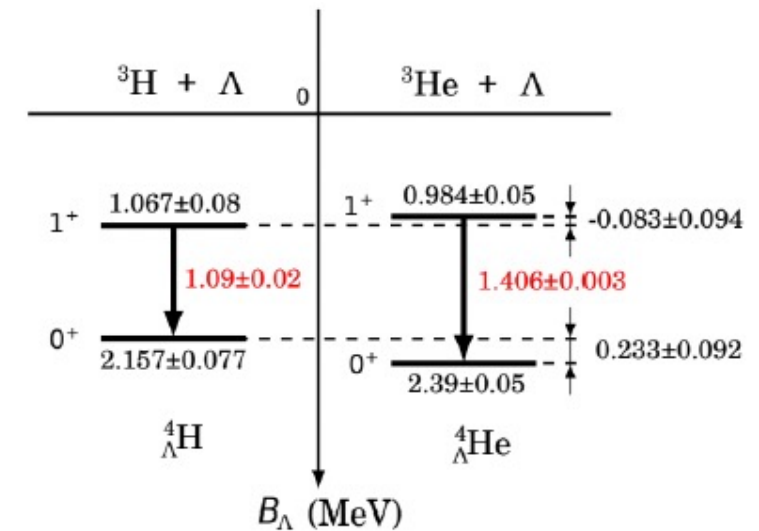
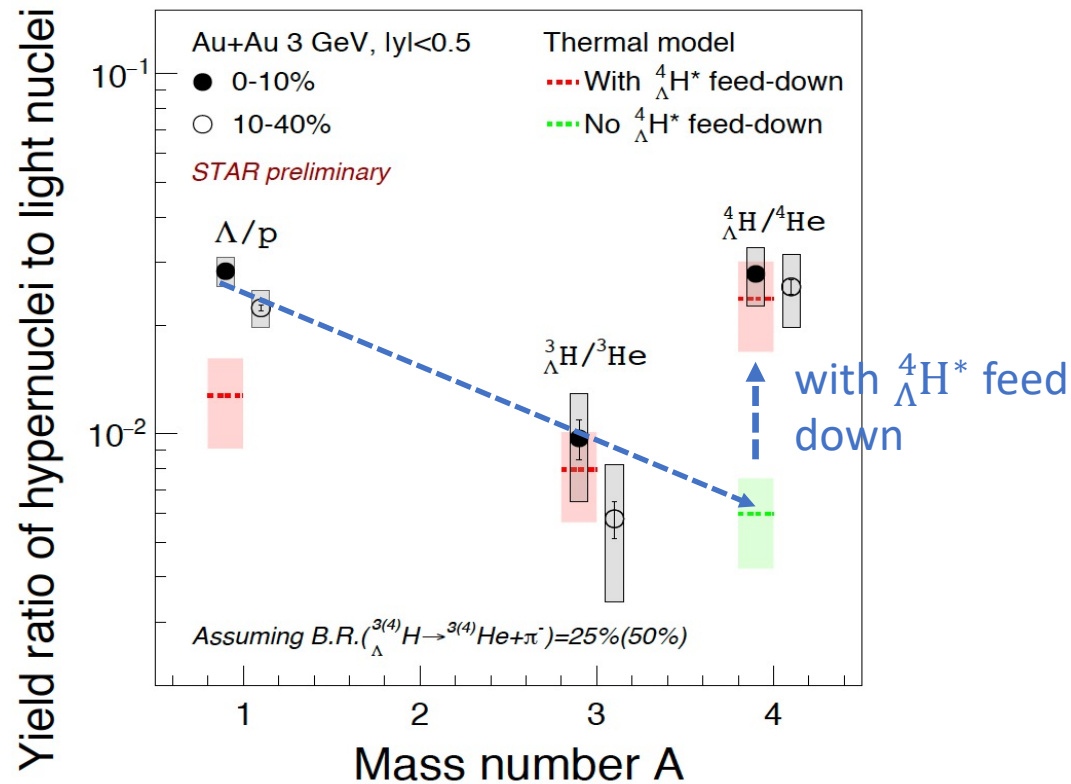
Mid-rapidity results qualitatively consistent with that the hypernuclei production is from **coalescence of hyperons and nucleons**.

Feeddown Contribution from Excited states



- Thermal model calculation, including excited ${}^4_\Lambda\text{H}^*$ feed down, shows a similar trend as data.

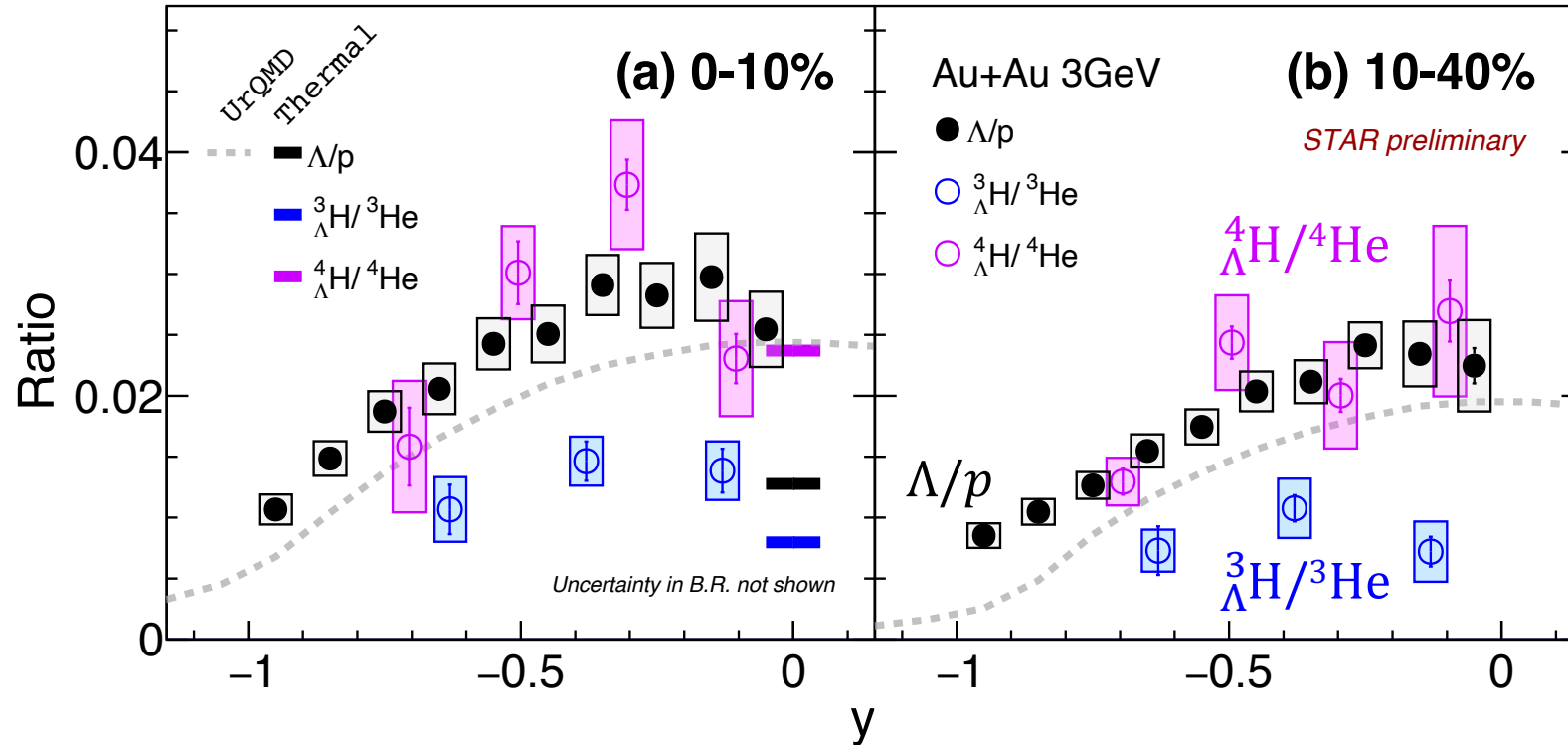
Data support the creation of excited $A=4$ hypernuclei in heavy ion collisions.



$${}^4_\Lambda\text{H}^*(J^+ = 1) \rightarrow {}^4_\Lambda\text{H}(J^+ = 0) + \gamma$$

A. Andronic et al, PLB 697, 203 (2011)
(updated, preliminary) (Thermal Model)

Hyper-to-light Nuclei Yield Ratios at 3 GeV



Note: ${}^3_{\Lambda}\text{H } R_3=27\%$,
 $B.R. ({}^4_{\Lambda}\text{H} \rightarrow {}^4\text{He } \pi^-) = 50\%$,
 uncertainties from B.R. not shown.

- ${}^3_{\Lambda}\text{H}/{}^3\text{He}$ yield ratios is lower than that of Λ/p at both 0-10% and 10-40% centrality in Au+Au collisions at $\sqrt{s_{NN}} = 3$ GeV.
- ${}^4_{\Lambda}\text{H}/{}^4\text{He}$ yield ratios are comparable to that of Λ/p .
 - Enhanced ${}^4_{\Lambda}\text{H}$ production indicates a significant excited state feed-down contributions.



Strangeness Population Factor

- Understand difference between $N-N$ and $Y-N$ interaction. S. Zhang et al, PLB 684, 224 (2010)

$$S_A = \frac{{}^A\Lambda H(A \times p_T)}{{}^A\text{He}(A \times p_T) \times \frac{\Lambda}{p}(p_T)} = \frac{B_A({}^A\Lambda H)(p_T)}{B_A({}^A\text{He})(p_T)}$$

$$E_A \frac{d^3 N_A}{dp_A^3} = B_A \left(E_{p,n} \frac{d^3 N_{p,n}}{dp_{p,n}^3} \right)^A \Big|_{\vec{p}_p = \vec{p}_n = \frac{\vec{p}_A}{A}}$$

Under some coalescence scenarios: PRC 99, 054905 (2019)

$$B_A = \frac{2J_A + 1}{2^A} \frac{1}{\sqrt{A}} \frac{1}{m_T^{A-1}} \left(\frac{2\pi}{R^2 + \left(\frac{r_A}{2}\right)^2} \right)^{\frac{3}{2}(A-1)}$$

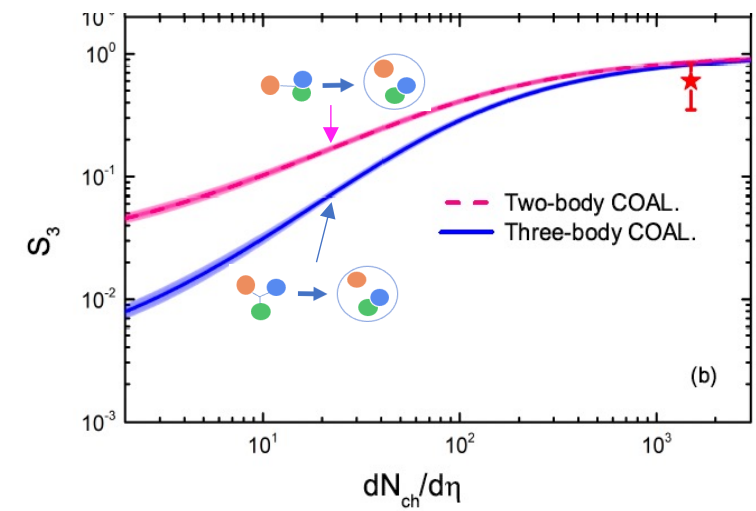
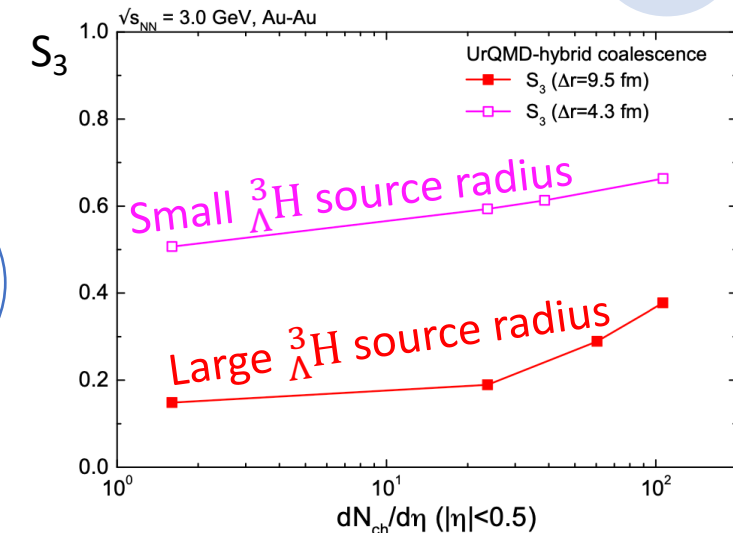
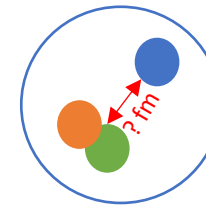
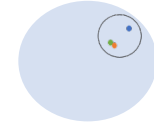
Source size
Radius

- Direct connection to coalescence parameters.
- Larger radius would have stronger source size dependence.
- Additional constrains on hypertriton structure.

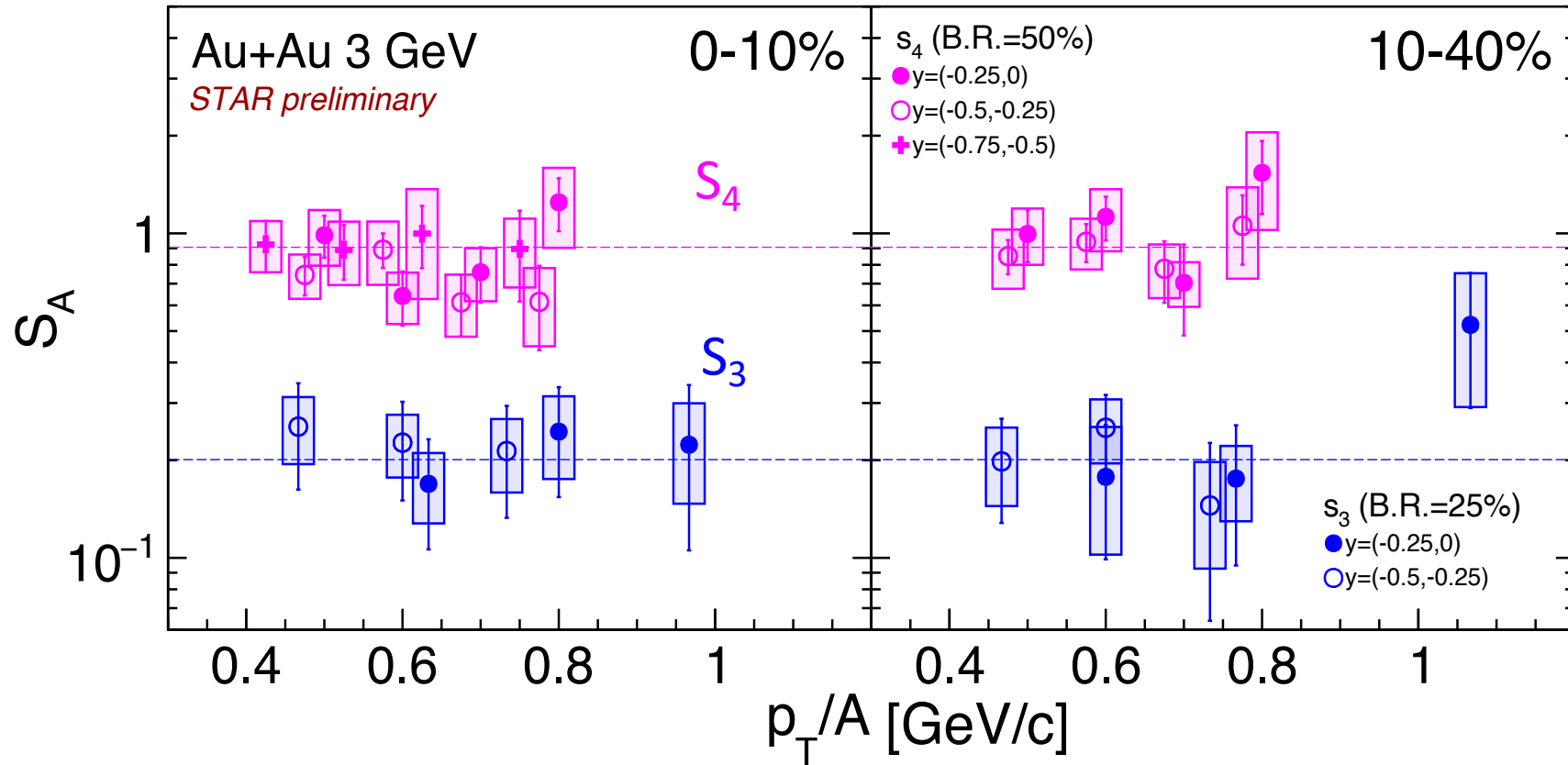
Small emitting source



Large emitting source



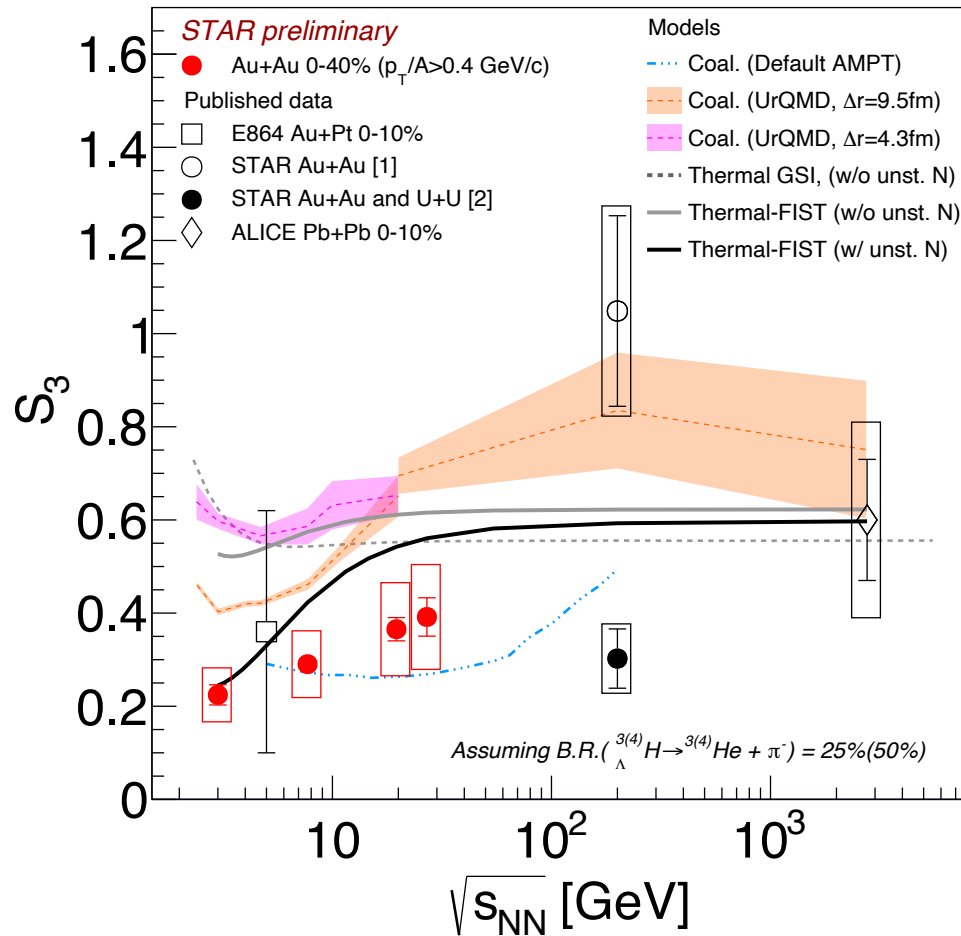
Strangeness Population Factor



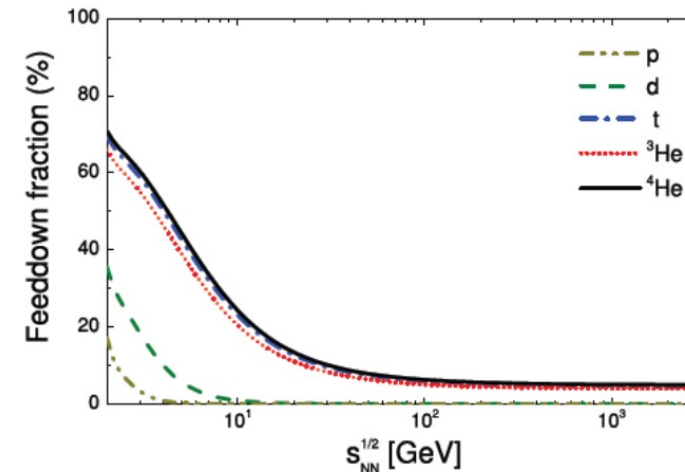
No obvious p_T , rapidity and centrality dependence of S_A observed at 3 GeV.

- Evidence that B_A of light and hypernuclei follow similar tendency versus p_T , rapidity and centrality.

Energy Dependence of S_3



- Increasing trend toward higher energies.
- Thermal-FIST calculations show that feed-down from unstable nuclei to light nuclei would lower S_3 in low energies.



Thermal-FIST calculations

STAR [2]: $0.7 < p_T/M < 1.5$ c

STAR [1]: Science 328, 58 (2010)

STAR [2]: arXiv:2310.12674 (2023)

Pb+Pb 2.76 TeV: ALICE, PLB 754,360 (2016)

Au+Pt 5 GeV: E864, PRC 70, 024902 (2004),

E864, J. Phys. Conf. Ser. 110, 032010 (2008)

A. Andronic et al, PLB 697 (2011)203 (Thermal GSI)

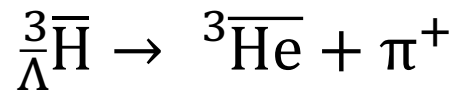
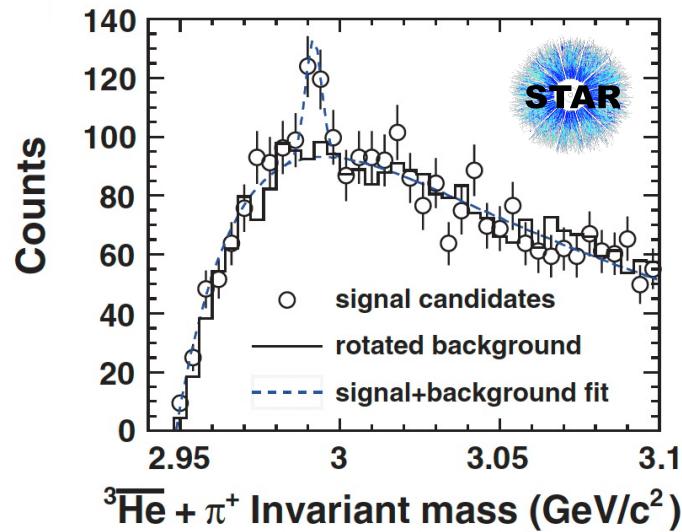
T. Reichert et al, PRC 107 (2023) 1, 014912 (UrQMD, Thermal-FIST)

S. Zhang et al, PLB 684(2010)224 (AMPT+coal.)

Anti-matter Hypernuclei

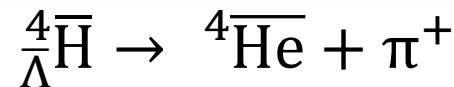
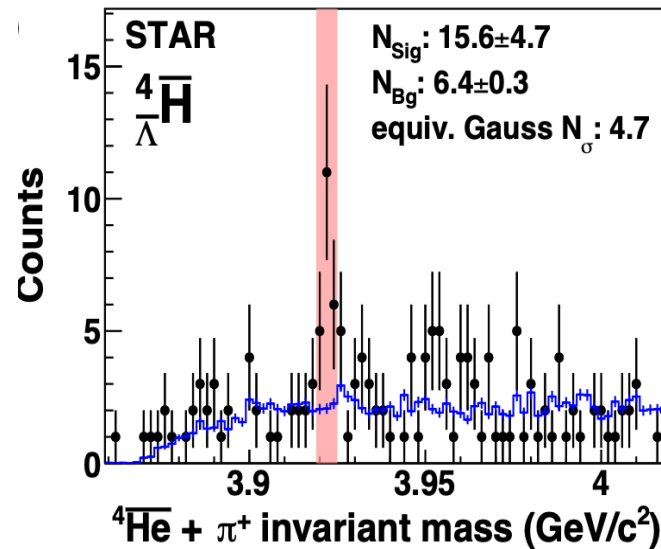
- STAR observed ${}^4_{\Lambda}\bar{\text{H}}$ in 2023.
 - The **heaviest observed antimatter** nuclear and hypernuclear cluster to date.
 - Benefit from high energy heavy ion collisions where $\mu_B \rightarrow 0$.
- **Lifetime of ${}^4_{\Lambda}\text{H}$ and ${}^4_{\Lambda}\bar{\text{H}}$ are consistent within uncertainties.**

${}^3_{\Lambda}\bar{\text{H}}$ was observed in 2010

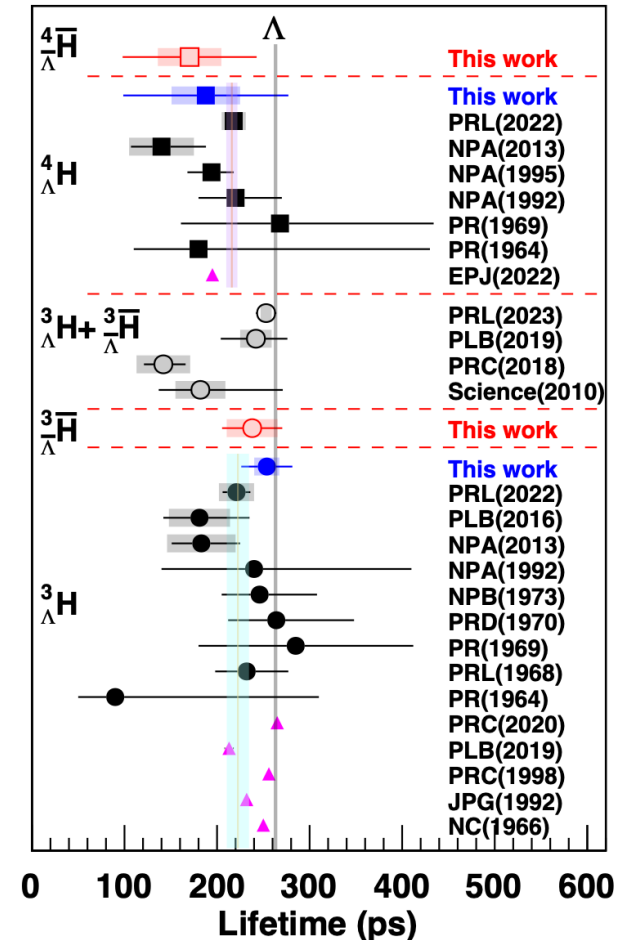


Science 328 (2010) 58-62

Discovery of A=4 anti-hypernuclei



arXiv:2310.12674, submitted to Nature



Summary

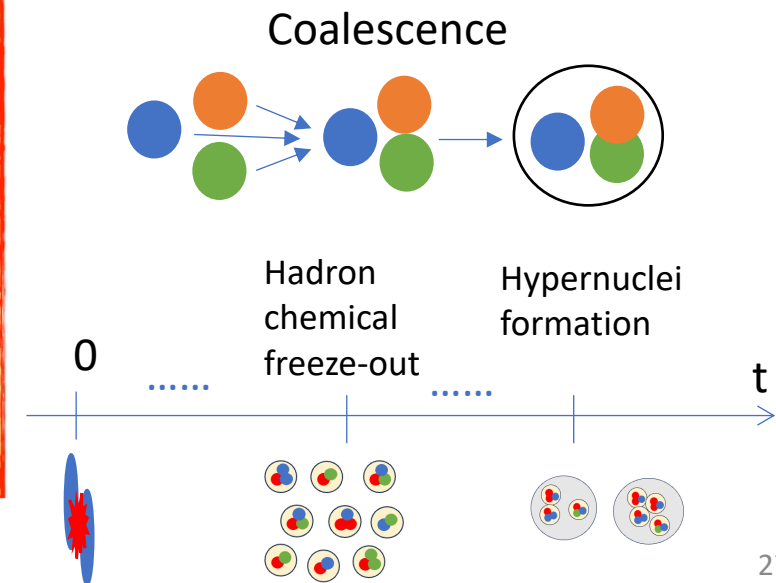


What we have measured:

- Properties: Lifetime of ${}^3_{\Lambda}\text{H}$, ${}^4_{\Lambda}\text{H}$ and ${}^4_{\Lambda}\text{He}$; ${}^3_{\Lambda}\text{H}$ R_3 .
- Collectivity and production yields:
 - The directed flow (v_1), mean p_T , dN/dy of ${}^3_{\Lambda}\text{H}$ and ${}^4_{\Lambda}\text{H}$ at $\sqrt{s_{NN}} = 3$ GeV.
 - ${}^3_{\Lambda}\text{H}$ excitation function from $\sqrt{s_{NN}} = 3$ -27 GeV at mid-rapidity.
- STAR discovered A=4 anti-matter hypernuclei.

Take home message:

- Hypernuclei are **abundantly produced** in heavy ion collisions!
- STAR data at 3 GeV support **coalescence mechanism** of hypernuclei formation at mid-rapidity.
- Hypernuclei **are not in equilibrium** at hadron chemical freeze-out at RHIC energies.



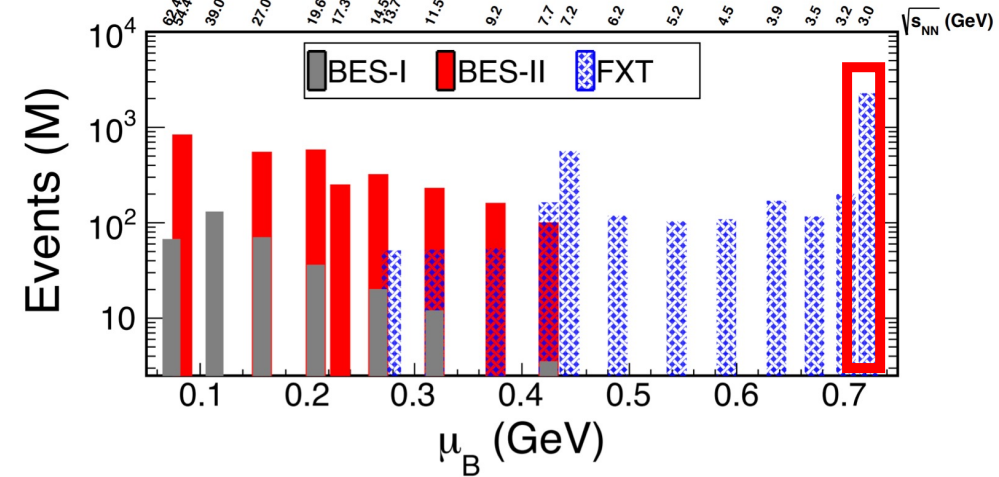
Future Perspective of Hypernuclei at STAR



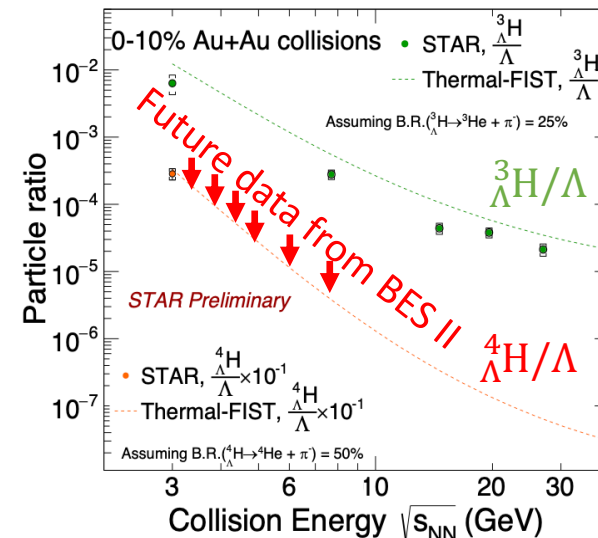
Huge datasets from BES-II and 200 GeV collisions.

- Precise measurements on hypernuclei **intrinsic properties**.
- Further investigation on **production mechanism**.
 - $A > 3$ hypernuclei.
 - Source size dependence.
- Search of **double Λ hypernuclei** ($Y - Y$ interaction).
 - e.g. $\Lambda\Lambda^4\text{He} \rightarrow \Lambda^4\text{He}\pi$, $\Lambda\Lambda^5\text{He} \rightarrow \Lambda^5\text{He}\pi$
- Precise measurements on **particle correlations**.
 - $p - \Lambda$, $d - \Lambda$, $\Lambda - \Lambda$ correlations.

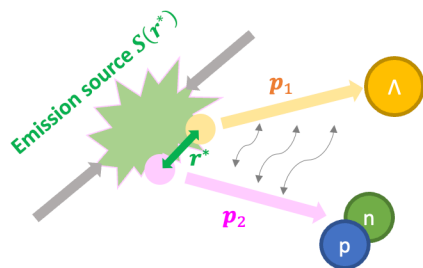
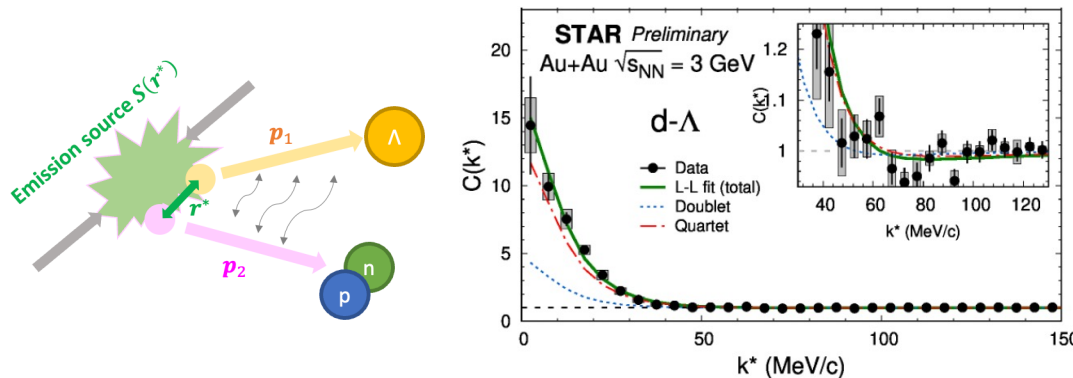
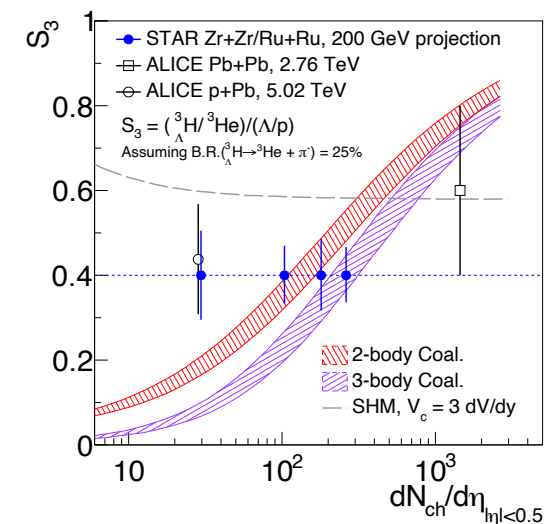
3 GeV 2B events!



$A\Lambda\text{H}/\Lambda$ vs energy



S_3 vs $dN/d\eta$



An aerial photograph of a tropical resort. In the center, a large, multi-story hotel building with a light-colored facade is situated on a peninsula. To the left of the hotel is a large, irregularly shaped lagoon with clear, turquoise water. A sandy beach runs along the coast between the hotel and the lagoon. The foreground and middle ground are filled with numerous palm trees and lush greenery. In the background, the ocean extends to the horizon under a clear blue sky. The overall scene is bright and sunny, suggesting a warm climate.

Thank you!